

# *Studies on Growth Kinetics of Nanoparticles Formation In Bulk Solution*

*A Project submitted to the  
National Institute of Technology, Rourkela*

*In partial fulfilment of the requirements  
for*  
**Bachelor of Technology (Chemical Engineering)**

*By*

**Subhasish Panigrahi**  
**Roll No. 10600028**

Under the guidance of  
**Dr. Santanu Paria**



**DEPARTMENT OF CHEMICAL ENGINEERING  
NATIONAL INSTITUTE OF TECHNOLOGY, ROURKELA  
ORISSA -769008, INDIA  
2010**



DEPARTMENT OF CHEMICAL ENGINEERING  
NATIONAL INSTITUTE OF TECHNOLOGY,  
ROURKELA -769 008, INDIA

---

## CERTIFICATE

The project report entitled “**Studies on growth kinetics of nanoparticles formation in bulk solution**”, submitted for the partial fulfilment for the degree of Bachelor of Technology in Chemical Engineering, National Institute of Technology, Rourkela.

SUBHASISH PANIGRAHI  
Roll. No-10600028

Dr. S. Paria  
Department of Chemical Engineering  
National Institute of Technology  
Rourkela - 769008  
INDIA

## ACKNOWLEDGEMENT

It is with a feeling of great pleasure that I express my most sincere heartfelt gratitude to **Dr. Santanu Paria** for suggesting the topic for my project and for his ready and able guidance throughout the course of preparing this report. I am greatly indebted to him for constructive suggestions and criticism from time to time during the progress of my work.

I thank the staff members of my department for their invaluable help and guidance. I owe a depth of gratitude to Prof. S. K. Agarwal, H.O.D, Department of Chemical Engineering, for all the facilities provided during the course of my tenure and for giving me good suggestions and encouraging me during my work. A special thanks to my Ph.D seniors Mr. Rajib Ghosh Chaudhury, Mr. Nihar Ranjan Biswal and Mr. Menaketan Ray for helping me and giving me good suggestions during my project work. Lastly, I thank all my class mates, who have helped me in some form or the other in the completion of my report.

**N.I.T. Rourkela**

**Date:**

**SUBHASISH PANIGRAHI**  
**Roll No: 10600028**

# CONTENTS

CERTIFICATE		ii
ACKNOWLEDGEMENT		iii
ABSTRACT		vi
CONTENTS		iv
LIST OF FIGURES		vii
NOMENCLATURE		ix
<b>CHAPTER 1</b>	<b>INTRODUCTION</b>	<b>1-6</b>
1.1	Introduction	1
1.2	History	1
1.3	Methods for synthesis of nanoparticles	2
1.3.1	Sol-Gel Method	2
1.3.2	Microemulsion Method	2
1.3.3	Mechanochemical synthesis	3
1.3.3.1	Sonochemical Synthesis	4
1.3.3.2	Electrodeposition Synthesis	4
1.3.4	Chemical vapour deposition method	4
1.4	Application of nanoparticles	4
1.5	Application of sulfur nanoparticles	5
<b>CHAPTER 2</b>	<b>LITERATURE REVIEW</b>	<b>7-14</b>
2.1	Introduction	7
2.2	Nucleation	7
2.3	Mechanism of Growth	9
2.4	Theoretical background	10
2.5	Present Work	13

<b>CHAPTER 3</b>	<b>DEVELOPMENT OF THE MATHEMATICAL MODEL AND CALCULATION</b>	<b>15-25</b>
3.1	Development of mathematical model (LSW Model)	15
3.1.1	Basic assumptions	15
3.1.2	Formulation	15
3.2	Mathematical model using Solvent-shift method	22
3.2.1	Basic assumptions	22
3.3	Sample calculation (LSW approach)	23
3.4	Sample calculation (Solvent shift approach)	24
<b>CHAPTER 4</b>	<b>RESULTS AND DISCUSSIONS</b>	<b>26-38</b>
4.1	Effect of different parameters on growth kinetics based on LSW Model.	26
4.1.1	Effect of concentration on growth kinetics.	26
4.1.2	Effect of temperature on growth kinetics.	27
4.1.3	Effect of surface energy on growth kinetics.	28
4.2	Effect of different parameters on growth kinetics based on Solvent-Shifting Model.	29
4.2.1	Effect of mass concentration on growth kinetics.	29
4.2.2	Effect of number density on growth kinetics.	30
4.3	Comparison between theoretical and experimental datas.	30
4.3.1	Comparison between experimental and theoretical datas Of effect of concentration on growth kinetics.	30
4.3.2	Comparison between the experimental and theoretical datas of effect of temperature on growth kinetics.	35
4.4	Error discussion.	37
<b>CHAPTER 6</b>	<b>CONCLUSION</b>	<b>39</b>
6.1	Conclusion.	39
<b>REFERENCES</b>		<b>40-43</b>

## **ABSTRACT**

Nanoparticles are gaining lots of importance recently due to their exciting applications in different fields like biomedical, pharmaceutical, electronics etc. In this report we studied the mechanism of nucleation and growth of formation of sulfur nanoparticles in aqueous medium. The main objective of this project is to study the effect of various parameters on the growth rate on the basis of size distribution of sulfur nanoparticles. The sulfur nanoparticles were prepared by acid catalyzed precipitation reaction from sodium thiosulphate. The growth rate of the particle depends on various factors, such as reactant concentration, acid to reactant ratio, diffusivity of the sulfur molecules, and temperature of the reaction and surface energy of the particles. As the sulfur nanoparticles are formed by precipitation reaction, the overall process can be divided into nucleation, growth and particle agglomeration. For this reaction nucleation is very fast. Actually as the reaction rate is very fast the growth rate mainly depends on the diffusion of the newborn particle from the bulk phase to the surface of the nuclei. So this is a diffusion limited growth reaction and mainly depends on diffusivity of the particle. The effect of different parameters on the growth rate of the formation of sulfur nanoparticles is studied by using the mathematical model derived by Lifshitz, Slyozov and Wagner and using LSW theory and also the results are compared with the experimental values of the size distribution of the formation of sulfur nanoparticles in aqueous medium.

***Key words:*** Sulfur nanoparticles, Nucleation, Growth, and Diffusion limited growth.

## LIST OF FIGURES

<b>FIGURE NO.</b>	<b>DESCRIPTION</b>	<b>PAGE NO.</b>
Figure.2	LaMer's Diagram (Concentration vs. Time).	8
Figure.3 (a)	The profile of solute concentration in a diffusion layer.	15
Figure.3 (b)	The diffusion layer around a spherical particle.	15
Figure.4.1	Effect of different reactant concentrations on growth kinetics at 298K.	26
Figure.4.2	Effects of different temperatures on growth kinetics at 5mM concentration.	27
Figure.4.3	Effect of surface energy on growth kinetics at 10mM concentration.	28
Figure.4.4	Effect of mass concentration on growth kinetics at 300K temperature.	29
Figure.4.5	Effect of number densities on growth kinetics at 300K temperature.	30
Figure.4.6	Comparison of the theoretical and experimental effect of 0.5mM reactant concentration on growth kinetics at 298K.	31
Figure.4.7	Comparison between theoretical and experimental effect Of 1mM reactant concentration at 298K temperature.	32
Figure.4.8	Comparison between experimental and theoretical effect of 5mM concentration on growth kinetics at 298K.	33
Figure.4.9	Comparison between experimental and theoretical effect of 10mM reactant concentration on growth kinetics at 298K	34

Figure.4.10	Comparison between the theoretical and experimental effect of 288K temperature on growth kinetics at 5mM reactant concentration.	35
Figure.4.11	Comparison between the theoretical and experimental Effect of 301K temperature on growth kinetics at 5mM Reactant concentration.	36
Figure.4.12	Comparison of experimental and theoretical effect of 315K temperature on growth kinetics at 5mM reactant Concentration.	37



## NOMENCLATURE

$x$	radius at any time, m
$K_d$	1 <sup>st</sup> order decomposition rate constant, s <sup>-1</sup>
$V_m$	molar volume, m <sup>3</sup> kmol <sup>-1</sup>
$J$	flux, kmol m <sup>-2</sup> s <sup>-1</sup>
$D$	diffusion coefficient, m <sup>2</sup> s <sup>-1</sup>
$\delta$	thickness of the diffusion layer, m
$C_A$	concentration at the interface, kmol m <sup>-3</sup>
$C_B$	concentration at the bulk phase, kmol m <sup>-3</sup>
$C_R$	solubility of the particle with radius 'r'
$C_\infty$	equilibrium concentration at the flat surface ( Bulk solubility)
$\sigma$	interfacial energy, J m <sup>-2</sup>
$R$	universal gas constant, kg m <sup>2</sup> kmol <sup>-1</sup> s <sup>-2</sup> k <sup>-1</sup>
$T$	temperature, k
$K$	coarsening constant, m <sup>3</sup> s <sup>-1</sup>
$K_B$	Boltzmann's constant, J k <sup>-1</sup>
$\eta$	viscosity of water, kg m <sup>-1</sup> s <sup>-1</sup>
$r$	atomic radius, m
$N$	number density, m <sup>-3</sup>

# CHAPTER 1

## Introduction

### 1.1 Introduction

In nanotechnology, a particle is defined as a small object that behaves as a whole unit in terms of its transport properties. Mainly, nanoparticles are sized in between 1 to 100 nanometers in all the three dimensions. Generally, nanoparticles are considered as an invention of modern science. Nanoparticles are of great scientific interest as they are effectively acting as a bridge between bulk materials and atom or molecular structures. Bulk materials have constant physical properties regardless of its size, but at the nano-scale this is totally an opposite case. Size dependent properties are observed such as quantum confinement in semiconductor particles, surface plasmon resonance in some metal particles and superparamagnetism in magnetic materials. The properties of the materials change as their size approaches the nano dimension and as the percentage of atoms at the surface becomes significant. For bulk materials larger than one micrometer the percentage of atoms at the surface is minuscule relative to the total number of atoms of the materials. The interesting and sometimes unexpected properties of nanoparticles are partly due to the aspects of the surface of the material dominating the properties in lieu of the bulk properties. Nanoparticles have a very high surface area to volume ratio. This provides a tremendous driving force in diffusion, especially at elevated temperatures and this also provides a large number of molecules for interaction. Sintering can take place at lower temperatures, over shorter time scales than for larger particles. This is theoretically does not affect the density of final product, though flow difficulties and the tendency of nanoparticles to agglomerate complicates matters. The large surface area to volume ratio also reduces the incipient melting temperature of nanoparticles (Buffat et al., 1976).

### 1.2 History

The first use of the concepts in ‘nanotechnology’ was in “There’s Plenty of Room at the Bottom”, the talk given by physicist Richard Feynman at an American Physical Society meeting at Caltech on December 29, 1959. Feynman described a process by which the ability to manipulate individual atoms and molecules might be developed, using one set of precise

tools to build and operate another proportionally smaller set, and so on down to the needed scale. He also noted that scaling issues would arise from the changing magnitude of various physical phenomena: gravity would become less important, surface tension and Vander Waals attraction would become increasingly more significant, etc. This basic idea appeared plausible, and exponentially assembly enhances it with parallelism to produce a useful quantity of end products. The term “nanotechnology” was defined by Tokyo Science University Professor Norio Taniguchi in 1974 and according to him “Nano-technology” mainly consists of the processing of, separation, consolidation and deformation of materials by one atom or by one molecule. In the 1980s the basic idea of this definition was explored in much more depth by Dr. K. Eric Drexler, who promoted the technological significance of nano-scale phenomena and devices through speeches the books *Engines of Creation: The Coming Era of Nanotechnology* (1986). Nanotechnology and nano-science got started in the early 1980s with two majors’ developments; the birth of cluster science and the invention of scanning tunnelling microscope (STM). This development led to the discovery of fullerenes in 1985 and carbon nano-tubes a few years later. In another development, the synthesis and properties of semiconductor nano-crystals was studied; this led to a fast increasing number of metal and metal oxide nanoparticles and quantum dots. The atomic force microscope (AFM or SFM) was invented six years after the STM was invented.

### **1.3 Methods for the synthesis of nanoparticles**

There are various methods used for the synthesis of nanoparticles. These methods are as follows;

#### **1.3.1 Sol-Gel Method**

The sol-gel process is a wet-chemical technique, it is also known as chemical solution deposition method widely used in the fields of materials science and ceramic engineering. These methods are mainly used for the fabrication of materials, mainly like metal oxide particle synthesis starting from a chemical solution (sol, short for solution) which acts as the precursor for an integrated network (or gel) of either discrete particles or network polymers (Brinker et al., 1990). Sol-gel approach is a cheap and low-temperature technique that controls the product’s chemical composition. Even small quantities of dopants, such as organic dyes and rare earth metals, can be introduced in the sol and end up uniformly dispersed in the final product. It can be also used in ceramics processing and manufacturing as an investment casting material, or as a means of producing very thin films of metal oxides for various purposes. Sol-gel derived materials have various applications in optics,

electronics, energy, space, biosensors, medicine and separation technology (Klein et al., 1994; Corriu et al., 2009).

### **1.3.2 Microemulsion Method**

In microemulsion method particle size can be controlled exactly. Microemulsion is a mixture of oil and aqueous phase with surfactant and cosurfactant. In microemulsion surfactants are formed reverse micelles and cosurfactant reduce the electrostatic repulsion force between the surfactant molecules. For particle formation, reagents are added in aqueous phase. Here micelles help in nucleation and growth of nanoparticles. By changing the molar ratio of water to surfactant, particle size and morphology can be controlled.

Xie et al. (2009) have prepared nano sulfur particles from sublimed sulfur. They added cystine solution drop wise to the sulfur ethanol saturated solution with ultrasonic treatment and cystine nano sulfur solution was obtained. The size of the cystine nano sulfur were around 50-100nm. Deshpande et al. (2008) have prepared sulfur nanoparticles using biodegradable iron chelate catalyst in reverse microemulsion method. They obtained rhombic sulfur of average particle size 10nm. Wang et al. (2006) prepared sulfur nanoparticles from sodium polysulfide by acid catalysis in reverse microemulsion method. They obtained monoclinic sulfur of average particle size 20nm. In this method polysulfide is the source of sulfur but for polysulfide synthesis nano sulfur is required and this problem is also same for Xie et al.(2009).

### **1.3.3 Mechanochemical synthesis**

This is a technique, where both mechanical force and chemical treatment are applied for nanoparticles synthesis. Chemical reactions occur at the interfaces of the nano-meter-sized grains that are continuously re-generated during milling (Koch et al., 1992). The reactions can occur either in a steady state manner or self-propagating combustive manner (Takacs et al., 1996; Shaffer et al., 1990). The reaction that occurs in a self-propagating combustive manner results in micron-sized particles due to high temperature, while the reactions that occur in a steady state manner result in a nano-sized particle is formed (Ding et al., 1995). So, to avoid self-propagating combustion, appropriate selection of milling parameters to reduce collision energy and by addition of inert diluents to the starting powder mixture to reduce the reaction rate is required. By selecting suitable conditions such as chemical reaction paths, stoichiometry of starting materials and milling conditions, mechanochemical processing can

be used to synthesise nano-crystalline particles dispersed within a soluble salt matrix. Selective removal of the matrix phase by washing the resulting powder with appropriate solvents can yield nanoparticles of the desired phase as small as 5 nm (McCormick et al., 2001). A wide range of nanoparticles have been synthesised by mechanochemical processing. There are mainly two types of mechanical force are used for particle synthesis, these are

### **1.3.3.1. Sonochemical Synthesis**

Sonochemical method has been widely used to fabricate nanoparticles with special structures. The chemical effects of ultrasonic sound arise from acoustic cavitations. That is the formation, growth and implosive collapse of bubbles in a liquid can drive many chemical reactions (Dierking et al., 1997; Kosbar et al., 1997). Hence it offers a very attractive method for the preparation of nanoparticles with different morphologies, including metals and oxides (Rajaram et al., 1995; Hudson et al 1998). The advantage in the ultrasound irradiation to the synthesis of mesoporous materials is a drastic reduction in fabrication time and the ability to induce aggregation of nanoparticles into porous structures without destroying the micellar structure. Sonication frequency range is 20 kHz to 1 MHz

### **1.3.3.2. Electrodeposition Synthesis**

Formation of shell over the core with charged polymers and inorganic materials can be carried out by this method in presence of electrical potential. In general, electric field is varied like a wave with positive and negative cycle. The metal deposits on the core surface during negative cycle and charged polymer deposits during the positive cycle.

### **1.3.4 Chemical vapour deposition method**

Chemical vapor deposition (CVD) is a chemical process used to produce high-purity, high-performance solid materials. The process is often used in the semiconductor industry to produce thin films. In a typical CVD process, the substrate is exposed to one or more volatile precursors, which react or decompose on the substrate surface to produce the desired deposit. Frequently, volatile by-products are also produced, which are removed by gas flow through the reaction chamber. Chemistry vapour deposition (CVD) was used in the preparation of nano-sulfur under severe conditions (Yang et al., 2003).

## **1.4 Application of Nanoparticles**

- Nanoparticles are used in paints, coatings and fillers.
- Drug delivery - Nanoparticles for absorption through the skin, eyes and for inhalation, to avoid stomach enzymes, which fortunately don't exist in the lungs, destroying drugs nano-capsules for delayed release; and dendrimers for drug delivery.
- Solar energy - Efficient solar cells are already developed by using nanoparticles and with the promise of drastic cost reductions on the horizon. Some will even produce hydrogen. Nanoparticles on the cell has been increased the cell power output by 67% in the ultraviolet range and about 10% in visible range (Choy et al., 2004).
- Nanoparticles are also used in Fuel cells.
- Display technologies and e-paper - A competitive area, with e-paper and carbon nanotube based field emission displays expected to be slugging it out with liquid-crystal displays.
- Nano-tubes – Both used as raw materials and as products. Multi-walled nano-tubes, the cheap and dirty kind, are already going into composites for increasing conductivity at much lower filler loads. Single-walled nano-tubes will have a much bigger effect in the longer term.
- Catalysis – Nanoparticles are also used as catalyst.
- Nano-composites - Mainly clay-based for structural applications (increased strength) or with novel properties. These are already used in automotive and aerospace industries.
- Storage technologies – It is also used for developing nano-tube RAM and terabyte hard drives.
- Nano-crystalline bulk materials or steels containing nano-particulates - some industries are using steel with nano-particulate carbon added during the rolling process.
- Coatings – Due to some its special properties, such as electro-chromic and self-cleaning properties, nanoparticles are used in coatings.
- Sensors - Bio and chemical sensors made from nano-wires and nano-tubes because of high sensitivity of nanoparticles to any chemicals.
- Bio-analysis - Devices using atomic force microscopes and quantum dots are already being readied for market.
- Textiles – Nano-fibres in stain-resistant trousers are already available.

## **1.5 Application of Sulfur Nanoparticles**

Sulfur is a biologically active element. The sulfur and sulfur containing compounds presented various biological activities such as removal of heavy metals, radical-scavenging,

antimicrobial activity, antioxidant and antitumor activities (Seokwon et al., 2006; Robert et al., 2003). The shape and size of sulfur particles are important factors affecting their properties and applications. Sulfur nanoparticles are paid much attention in the field of science and technology and their applications in chemistry and biochemistry have aroused some chemists' interest. In the area of agricultural field sulfur is used as fungicide against the apple scab disease under colder conditions (Ellis et al., 1998). Nano size sulfur particles also have many important applications like pharmaceutical, synthesis nano composites for lithium batteries (Zheng et al., 2006; Yong et al., 2007).

# CHAPTER 2

## Literature Review

### 2.1 Introduction

The fundamental study on kinetics of precipitation reaction is important to improve the industrial precipitation process. The precipitation reaction is a combination of two stage process, nucleation and growth. Nucleation plays an important role in controlling the properties of the final product, size distribution and nature of the phase. Precipitation reaction is only the phase transformation from liquid to solid with chemical reaction. According to classical theory nucleation is a minimization process in terms of energy of the overall system. Whenever particles are generated from the homogeneous liquid mixture, a new solid liquid interfacial area is generated with a specific surface energy proportional to the square of its radius. Whereas, considering the bulk energy, due to the formation of the solid, the energy gained is proportional to the cube of the particle radius. These two energy terms are opposite in nature. The change in total energy is mainly due to the contribution of these two, but some other factors like, motion of the particles in the medium, electrostatic contribution and total energy. In case of precipitation reaction initially, surface energy dominates the total energy and the reaction become unfavorable. Nucleation and growth of sulfur solution formation is extensively studied by V. K. LaMer and co-workers (LaMer, 1947; 1950; 1952) and developed the mechanism of formation of nano crystals or colloids from a homogeneous supersaturated aqueous medium. According to them, in a short time period nucleation process is completed and the particles having larger size than critical radius started to grow. The growth process is controlled by either diffusion or surface reaction.

### 2.2 Nucleation

Nucleation is the process by which atoms (or ions) that are free in solution come together to produce a thermodynamically stable cluster. The cluster must exceed a specific size (the critical size) determined by the competition between the aggregate curvature (Laplace pressure) and the free energy favouring the growth of the new phase. Once the critical size is exceeded, the cluster becomes a supercritical nucleus capable of further growth. If the nucleus is smaller than the critical size, spontaneous dissolution can occur (Tojo et al., 2006).



LaMer et al. (1950) have studied extensively nucleation and growth in sulfur solutions, from which they developed an understanding of the mechanism for the formation of colloids or nanocrystals from a homogeneous, supersaturated medium. Their mechanism suggested that a synthesis of the colloid should be designed in such a way that the concentration increases rapidly, rising above the saturation concentration for a long period, when a short burst of nucleation occurs with the formation of a large number of nuclei in a short space of time. These particles grow rapidly and lower the concentration below the nucleation level whilst allowing the particles to grow further at a rate determined by the slowest step in the growth process, thus separating the nucleation and growth in time. LaMer's mechanism is depicted schematically by means of the simple diagram shown in fig.3.1. The requirements for monodispersity, as evident from LaMer's diagram, are a high rate of nucleation leading to the burst of nuclei formation in a short period, an initial fast rate of growth of these nuclei to reduce the concentration below the nucleation concentration rapidly and an eventual slow rate of growth leading to a long growth period compared to the nucleation period.

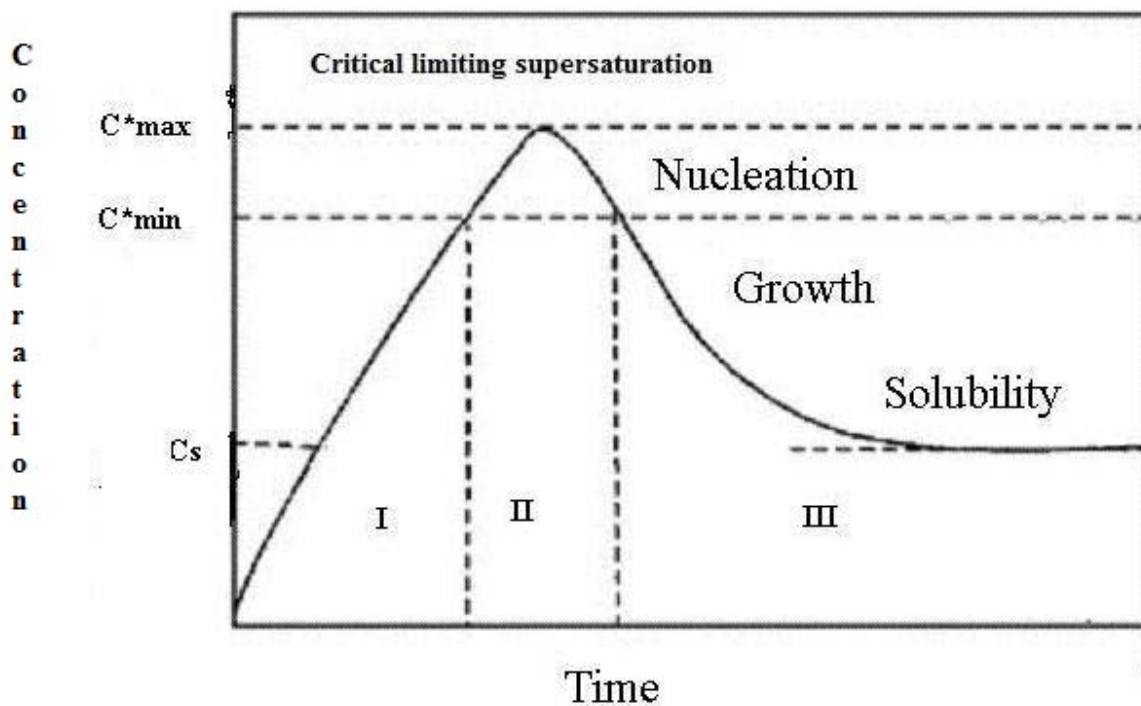


**Fig.2. LaMer's Diagram (Concentration vs. Time). (LaMer et al., 1950).**

They also derived the rates of growth of solutions prepared by this method. This diagram (fig.2) illustrates the variation of the concentration with time during a precipitation reaction and is based on the principle that the nucleation is the limiting step in the precipitation reaction. In the first step, the concentration increases continuously with increasing time. As

the concentration reaches the critical super saturation value, nucleation occurs. This leads to a decrease of the concentration. Between the concentrations  $C_{\max}^*$  and  $C_{\min}^*$  the nucleation occurs. Later, the decrease of the concentration is due to the growth of the particles by diffusion. This growth occurs until the concentration reaches the solubility value. This model has been applied to the microemulsion medium, i.e., that nucleation occurs in the first part of the reaction and later only growth of the particles occurs. If this model is followed, the size of the particles will increase continuously with the concentration of the precursor or a minimum in the variation of the size with the concentration can also be expected. This stems from the fact that the number of nuclei is constant and the increase of concentration leads to an increase of the size of the particles (Destree et al., 2006).

### **2.3 Mechanism of Growth**

Nucleation occurs over sometime with constant monomer concentration. Eventually surface growth of clusters begins to occur which depletes the monomer supply. When the monomer concentration falls below the critical level for nucleation, nucleation ends. A general analysis of the growth process is then important to understand nanocrystal synthesis. In general, the surface to volume ratio in nanoparticles is quite high. As a result of the large surface area present, it is observed that surface excess energy becomes more important in very small particles, constituting a non negligible percentage of the total energy. Hence, for a solution that is initially not in thermodynamic equilibrium, a mechanism that allows the formation of large particles at the cost of smaller particles reduces the surface energy and hence plays a key role in the growth of nanocrystals. Coarsening effects, controlled either by mass transport or diffusion, are often termed the Ostwald ripening process. This diffusion limited Ostwald ripening process is the most predominant growth mechanism (Lifshitz et al., 1961; Wagner et al., 1961).

The diffusion process is dominated by the surface energy of the nanoparticles. The interfacial energy is the energy associated with an interface due to differences between the chemical potential of atoms in an interfacial region and atoms in neighboring bulk phases. For a solid species present at a solid-liquid interface, the chemical potential of a particle increases with decreasing particle size, the equilibrium solute concentration for a small particle is much larger than for a large particle, as described by the Gibbs-Thompson equation. The resulting concentration gradients lead to transport of the solute from the smaller particles to larger

particles. The equilibrium concentration of the nano-crystal in the liquid phase is dependent on the local curvature of the solid phase. Differences in the local equilibrium concentrations, due to variations in curvature, set up concentration gradients and provide the driving force for the growth of larger particles at the expense of smaller particles (Sugimoto, 1987; Rao et al., 2007).

## **2.4 Theoretical background**

There are various model developed for the mechanism of the nanoparticles formation, these are as follows

Ethayaraja et al. (2008) have studied the model for core-shell nanoparticles formation by ion-exchange mechanism and stated that core-shell nanoparticles can be synthesized by partial exchange of the cation of the core nanoparticles by a second cation of the desired shell compound. Process time and cation concentration can be varied to control the thickness of the shell. They have developed a mathematical model that describes the process of ion-exchange from preformed spherical nanoparticles. The overall process consists of diffusion of the cation from the solution to the core-nanoparticles surface, then solid-state diffusion of the cation across the shell, and finally the cation exchange reaction. The reaction rate is very fast, so diffusion in the shell is the slowest step and also the rate-controlling step. This model was compared with the available experimental data of CdS-PbS core-shell nanoparticles formation at various  $[Pb^{2+}]/[Cd^{2+}]$  molar ratios and at different process times. The model can be useful for a priori specification of experimental conditions required for a desired shell thickness.

Mehra et al. (2006) have proposed shell growth mechanism to occur simultaneously with ion-exchange. This is a more general scheme by which they could explain the outer core-shell diameter. However, in their simulation, ion-exchange being still limited to only a monolayer formation, their scheme cannot explain complete conversion of a core nanoparticle to another nanoparticle of a different material, via the intermediate core-shell structure.

LaMer et al. (1945) have studied the kinetics of diffusion controlled molecular and ionic reactions in solution as determined by measurements of the quenching of fluorescence. Theory of chemical kinetics states that the absolute rate of reaction is determined by the concentration of activated complexes, in equilibrium with the reactants and products, and multiplied by the frequency with which these critical complexes decompose to form the end

products. In some of the rapid reactions like quenching of fluorescence by iodide ions, the rate controlling process is the diffusion of the reactants. Because of the condensed nature of liquids, collisions in solutions are complex as compared to gases. The reactants diffuse through the solution, as a result of thermal motion, and finally collide. The pair is surrounded by a cage of solvent molecules and in this manner is held in coordination so that reactants execute motion or vibration relative to each other. To calculate the reaction rate, they have considered one solution is at rest and another solution is moving towards it and diffusion occurs due to the thermal motion of the molecules. They have considered the forces acting between the molecules, diffusion force, friction force and electrical force. In their experiment, they have considered the effect of inter-ionic forces on the rate of diffusion. For the calculation, they have assumed the quencher as the centres of diffusion and the concentration of excited fluorescent molecules is taken to be zero on the surface of the quencher, due to the quenching. Finally, they have stated that quenching process, involves an encounter between a dye molecule excited by light absorption (fluorescein ion) and a quencher (iodide ion). Following the encounter, the energy of excitation is converted into thermal motion of the surrounding solvent molecules. A direct measurement of the time decay of fluorescence and also investigating quenching is too difficult for precision studies because of the extremely short half-life period.

LaMer et al. (1952) have studied the kinetics of the formation of the carbinol of crystal violet and they have stated that, the fading of crystal violet in the presence of hydroxyl ion follows quantitatively the Bronsted-Debye law for primary kinetic salt effects. Crystal violet obeys Beer's law at the wave length of maximum absorption. There is a strong specific solvent effect: the addition of acetone or dioxane to an aqueous solution of the dye produces a shift in the absorption peak of the crystal violet ion toward longer wave lengths and at low concentrations of organic solvents, produces an effect on the specific reaction rate which is opposite to that expected on the basis of the decrease in dielectric constant. The use of normalized rate constants does not improve the agreement with simple electrostatic theory. The energy of activation in acetone-water mixtures greater than in the case of water alone, at this ionic strength, contrary to the expected decrease due to the lowering of the coulombic activation energy in this reaction between oppositely charged ions produced by lowering the dielectric constant. The activation energy for the carbinol formation of malachite green is less than that for crystal violet. The higher rate constant of the former is due to reduction in activation energy, also to less negative entropy of activation. Sufficient alkali was employed

in these experiments to give reactions faster than this. So, in this experiment alkali consumption is more.

Keuren et al. (2003) have studied the growth kinetics of anthracene nanoparticles by using a method called 'solvent shift'. In this method they have reduced the solute solubility by changing the ratio of two components of a binary solvent to get super saturation quickly and initially, the particle size of the particles increased rapidly followed by much slower growth. They have used dynamic light scattering (DLS) for characterizing particles above 10 nm, and UV-VIS absorption spectroscopy to look at molecular arrangement. These measurements are performed both as functions of composition (ratio of water to acetone in the binary solvent) and as functions of time after changing the solubility. By correlating these results, they got an idea on the size and structure of the nanoparticles as functions of time and conditions during nucleation and growth. The nanoparticles formed in their systems, the super saturation condition is created initially and the system then allowed equilibrating. The growth of the particles is accompanied by the depletion of solute from the bulk solution, leading eventually to the end of the supersaturated condition. They have neglected the surface term in the free energy difference, which will mean the equilibrium concentration at the surface will have a dependence on the particle size. They have started with nucleation sites that are already larger than the critical size. In order to understand the growth of the particles, they have used a simple model describing the mass transport to the particle surface through diffusion, coupled to the decrease in bulk solute concentration. They have assumed that the growth of the particles is a diffusion-limited process. For the calculation part, they have taken the values of diffusivity coefficient and viscosity that are available in the theory.

Hale et al. (2005) have studied the growth kinetics and modelling of ZnO nanoparticles. They have used the Ostwald ripening process for study of the growth kinetics. They have used the Gibbs-Thomson equation and Fick's law for the derivation of the rate law. From the Ostwald ripening process, they have concluded that the formation of many small particles is kinetically favoured and the large particles are thermodynamically favoured. This is because small particles have a larger surface area-to-volume ratio than large particles and are consequently easier to produce. Molecules on the surface are energetically less stable than the ones already well ordered and packed in the interior. Large particles, with their greater volume-to-surface area ratio, therefore represent a lower-energy state. Hence, many small particles will attain a lower-energy state if transformed into large particles. They have used

the experimental values of solubility and hydrodynamic radius to calculate the diffusion coefficient from Stokes-Einstein equation and Ostwald model and then, compared the two models. They have calculated absorbance of a dilute solution of small particles from Mie theory and also used some dielectric properties.

Wong et al. (1998) have studied the growth kinetics of nanocrystalline ZnO particles from colloidal suspensions. Colloidal chemistry techniques were used to synthesize ZnO particles in the nanometre size regime. The particle kinetics was determined by monitoring the optical band edge absorption and using the effective mass model to approximate the particle size as a function of time. In this model, the higher curvature and the chemical potential of the smaller particles provide a driving force for dissolution. Particle sizes and Crystal structure identification were determined by using high-resolution transmission electron microscope and X-ray diffraction respectively. The concentration of  $Zn^{2+}$  in the colloidal suspensions was determined by atomic absorption spectroscopy of solution isolated from the ZnO particles by dialysis. They have noted that particle sizes of less than about 1.5 nm could not be obtained. For the particle growth kinetics they have used Ostwald ripening model and Stokes-Einstein equation and compared the two models. But in colloidal suspensions both diffusion and convection can contribute to ion motion.

Oskam et al. (2002) have studied the growth kinetics of  $TiO_2$  nanoparticles from titanium (IV) alkoxide at high Water/titanium ratio. The radius of primary particles was found to be between 1.5 and 8 nm, and the average particle radius cubed is shown to increase linearly with time in agreement with the Lifshitz-Slyozov-Wagner model for coarsening. The rate constant for coarsening increases with temperature due to the temperature dependence of the viscosity of the solution and the equilibrium solubility of  $TiO_2$ . At longer times and higher temperatures, secondary particles formed by epitaxial self-assembly of primary particles were observed with high-resolution transmission electron microscopy. The number of primary particles per secondary particle increases with time and the percentage of primary particles present in the colloid decreases with increasing temperature.

## **2.5 Present Work**

In this project, the mechanism of the formation of sulfur nanoparticles from sodium thiosulfate solution using oxalic acid in aqueous medium as a catalyst is studied. Here, we are

using two approaches that is LSW Model and another one is Solvent-Shift approach. By using this approach we are mainly studying the effect of various parameters on the growth kinetics of the particles. In LSW approach, the considered parameters are reactant concentration, temperature, diffusion coefficient and the surface energy. In Solvent-shift approach the varying parameters are mass concentration and the number density. In LSW approach diffusion is the slowest step and also the rate controlling step. Here, nanoparticles are formed mainly by diffusion and also model is developed by using the concept of Fick's first law of diffusion. But in Solvent-shift approach we are using the mass concentration of the solute. Some datas are taken from the literature available and these values are substituted in the mathematical model derived. New datas are generated from the model with respect to particle radius and time. Then, these generated values are compared with the experimental values and error is calculated with respect to the experimental values.

# CHAPTER 3

## Development Of The Mathematical Model and Calculation

### 3.1 Development of mathematical model (LSW Model)

The growth of nanocrystals in solution involves two important processes, the nucleation followed by the growth of the nanocrystals (Rao et al., 2007).

#### 3.1.1 Basic assumptions

The assumptions are made according to the LSW theory (Lifshitz et al., 1961; Wagner et al., 1961; Rao et al., 2007).

- Particles are assumed to be spherical in a supersaturated medium.
- The total mass of the solute is conserved.
- Assumptions of the particle being spherical are characterized only by the radius distribution.
- Processes such as nucleation and aggregation that introduce new particles are negligible.

#### 3.1.2 Formulation (Lifshitz et al., 1961; Wagner et al., 1961; Rao et al., 2007).

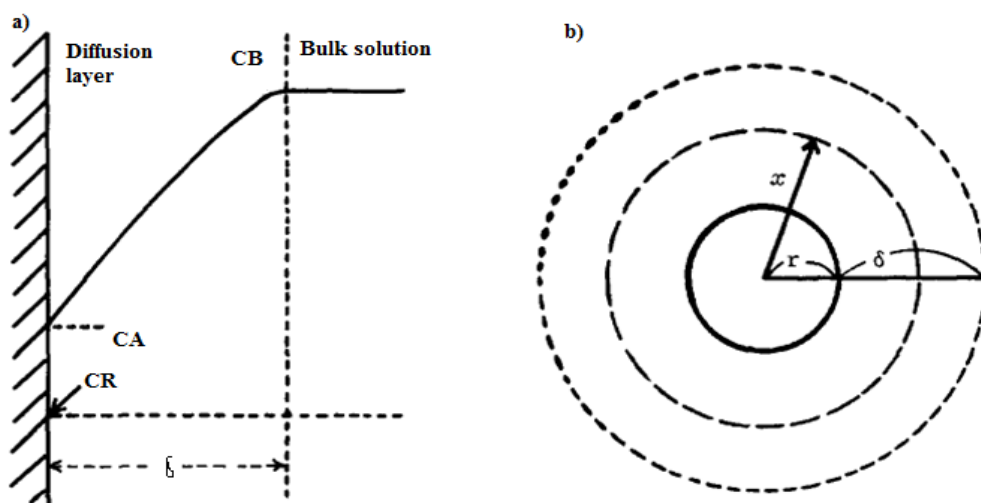


Fig.3 (a) The profile of solute concentration in a diffusion layer. (b) The diffusion layer around a spherical particle. (Sugimoto, 1987).



$x$  = Radius at any time

By using Fick's first law, the flux passing through a spherical surface with radius ' $x$ ' within the diffusion layer is

$$J = D \times 4\pi x^2 \times \frac{dc}{dx} \quad (3.1)$$

Where,

$J$  = Flux

$D$  = Coefficient of diffusion

$\frac{dc}{dx}$  = Concentration gradient

$\delta$  = Thickness of the diffusion layer

$C_A$  = Concentration at the interface

$C_B$  = Concentration at the bulk phase

At steady state,  $J$  is constant over the diffusion layer ' $x$ '. Here, diffusion of the molecules from interface to the bulk phase taken place. Then, solving the equation (3.1) and integrating with proper limits,

$$J \times \int_r^{r+\delta} \frac{dx}{x^2} = 4\pi D \int_{C_A}^{C_B} dc \quad (3.2)$$

$$J \left[ \frac{-1}{x} \right]_r^{r+\delta} = 4\pi D \int_{C_A}^{C_B} dc$$

$$J \left[ \frac{-1}{r+\delta} + \frac{1}{r} \right] = 4\pi D [C_B - C_A]$$

$$J \left[ \frac{1}{r} - \frac{1}{r+\delta} \right] = 4\pi D [C_B - C_A]$$

$$J \left[ \frac{r+\delta-r}{r(r+\delta)} \right] = 4\pi D [C_B - C_A]$$

$$J \left[ \frac{\delta}{r(r+\delta)} \right] = 4\pi D [C_B - C_A]$$

$$J = \frac{4\pi D (C_B - C_A) r (r + \delta)}{\delta} \quad (3.3)$$

The above flux is due to diffusion.

Another flux is due to the first order reaction at the surface. This flux can be equated to the consumption rate of the monomer species at the surface of the particles (Rao et al., 2007). So the flux due to the reaction is,

$$J = 4\pi r^2 \times K_d (C_A - C_R) \quad (3.4)$$

Where,

$K_d$  = First order decomposition rate constant

$C_R$  = Solubility of the particle with radius '  $r$  '

At steady state two fluxes (flux due to diffusion and reaction at the surface) are same.

Then

$$\frac{C_A - C_R}{C_B - C_A} = \frac{D}{rK_d} \left( \frac{r + \delta}{\delta} \right)$$

$$\frac{C_A - C_R}{C_B - C_A} = \frac{D}{rK_d} \left( 1 + \frac{r}{\delta} \right) \quad (3.5)$$

$$\text{Atoms in a crystal} = \frac{4\pi r^3}{3V_m} \quad (3.6)$$

$$\text{Rate of species entering, } J = \frac{d}{dt} \left( \frac{4\pi r^3}{3V_m} \right) \quad (3.7)$$

$$J = \frac{4\pi r^2}{V_m} \times \frac{dr}{dt}$$

$$\frac{dr}{dt} = \frac{JV_m}{4\pi r^2} \quad (3.8)$$

Where,

$$\frac{dr}{dt} = \text{Growth rate}$$

$$V_m = \text{Molar volume}$$

In solution, it is very difficult to measure  $C_A$ , so we have to eliminate  $C_A$  from the two equations (3.3) and (3.4).

$$J = 4\pi r^2 \times K_d (C_A - C_R)$$

$$C_A - C_R = \frac{J}{4\pi r^2 K_d}$$

$$C_A = \frac{J}{4\pi r^2 K_d} + C_R \quad (3.9)$$

Substituting the value of  $C_A$  in equation (3.3), we get

$$J = 4\pi Dr \left(1 + \frac{r}{\delta}\right) (C_B - C_A)$$

$$J = 4\pi Dr \left(1 + \frac{r}{\delta}\right) \left(C_B - \frac{J}{4\pi r^2 K_d} - C_R\right)$$

$$J \left(4\pi Dr \times \frac{J}{4\pi r^2 K_d}\right) \left(1 + \frac{r}{\delta}\right) = 4\pi Dr \left(1 + \frac{r}{\delta}\right) (C_B - C_R)$$

$$J \left(1 + \frac{D}{rK_d} \left(1 + \frac{r}{\delta}\right)\right) = 4\pi Dr \left(1 + \frac{r}{\delta}\right) (C_B - C_R)$$

$$J = \frac{4\pi Dr \left(1 + \frac{r}{\delta}\right) (C_B - C_R)}{\left(1 + \frac{D}{rK_d} \left(1 + \frac{r}{\delta}\right)\right)} \quad (3.10)$$

Substituting the value of  $J$  in equation (4), we get

$$\frac{dr}{dt} = \frac{4\pi D r \left(1 + \frac{r}{\delta}\right) (C_B - C_R) V_m}{\left(1 + \frac{D}{r K_d} \left(1 + \frac{r}{\delta}\right)\right) 4\pi r^2}$$

$$\frac{dr}{dt} = \frac{D \left(1 + \frac{r}{\delta}\right) (C_B - C_R) V_m}{r \left(1 + \frac{D}{r K_d} \left(1 + \frac{r}{\delta}\right)\right)} \quad (3.11)$$

According to Gibb's- Thompson equation

$$C_R = C_\infty e^{\left(\frac{2V_m\sigma}{rRT}\right)} \quad (3.12)$$

Where,

$C_\infty$  = Equilibrium concentration at the flat surface (Bulk solubility).

$\sigma$  = Interfacial energy

$R$  = Universal gas constant

$T$  = Temperature

Assuming that  $\frac{2V_m\sigma}{rRT}$  is very small, so neglecting the higher order terms in the series expansion, we get

$$C_R = C_\infty \left(1 + \frac{2V_m\sigma}{rRT}\right) \quad (3.13)$$

Similarly  $C_B$  can be written as

$$C_B = C_\infty \left(1 + \frac{2V_m\sigma}{r_B RT}\right) \quad (3.14)$$

Substituting the values of  $C_B$  and  $C_R$  in equation (3.11), we get

$$\frac{dr}{dt} = \frac{D\left(1 + \frac{r}{\delta}\right)(C_B - C_R)V_m}{r\left(1 + \frac{D}{rK_d}\left(1 + \frac{r}{\delta}\right)\right)}$$

$$\frac{dr}{dt} = \frac{D\left(1 + \frac{r}{\delta}\right)V_m\left[C_\infty\left(1 + \frac{2V_m\sigma}{r_B RT}\right) - C_\infty\left(1 + \frac{2V_m\sigma}{r RT}\right)\right]}{r\left(1 + \frac{D}{rK_d}\left(1 + \frac{r}{\delta}\right)\right)}$$

$$\frac{dr}{dt} = \frac{D\left(1 + \frac{r}{\delta}\right)2V_m^2\sigma C_\infty\left(\frac{1}{r_B} - \frac{1}{r}\right)}{rDRT\left[\frac{1}{D} + \frac{1}{rK_d}\left(1 + \frac{r}{\delta}\right)\right]}$$

$$\frac{dr}{dt} = \frac{2V_m^2\sigma C_\infty\left(1 + \frac{r}{\delta}\right)\left(\frac{1}{r_B} - \frac{1}{r}\right)}{rRT\left[\frac{1}{D} + \frac{1}{rK_d}\left(1 + \frac{r}{\delta}\right)\right]} \quad (3.15)$$

Mainly diffusion layer thicknesses are of the order of microns. So, in case of nano-crystal we assume,  $r \ll \delta$

So for  $r \ll \delta$ , equation (3.15) became

$$\frac{dr}{dt} = \frac{2V_m^2\sigma C_\infty\left(\frac{1}{r_B} - \frac{1}{r}\right)}{rRT\left(\frac{1}{D} + \frac{1}{rK_d}\right)} \quad (3.16)$$

This is a diffusion limited growth mechanism. In this case diffusion is the slowest step and also the rate controlling step and the particle growth is mainly controlled by the diffusion of the monomers to the surface (Lifshitz et al., 1961; Wagner, 1961).

So  $D \ll rK_d$

Then equation (3.16) reduces to

$$\frac{dr}{dt} = \frac{2V_m^2 D \sigma C_\infty \left( \frac{1}{r_B} - \frac{1}{r} \right)}{rRT}$$

$$\frac{dr}{dt} = \frac{2V_m^2 D \sigma C_\infty \left( \frac{r}{r_B} - 1 \right)}{r^2 RT}$$

$$\frac{dr}{dt} = K_D \times \frac{\left( \frac{r}{r_B} - 1 \right)}{r^2} \quad (3.17)$$

$$\text{Where, } K_D = \frac{2V_m^2 D \sigma C_\infty}{RT} \text{ (Constant)} \quad (3.18)$$

If the total mass of the system is kept conserved, the LSW theory showed that the ratio

$\frac{r}{r_B}$  is constant. So, then assuming  $\frac{r}{r_B}$  as constant, equation (3.17) reduces to,

$$\frac{dr}{dt} = \frac{K_D \times Const}{r^2} \quad (3.19)$$

$$\frac{dr}{dt} = \frac{K_C}{r^2}$$

$$\int_{r_0}^r r^2 dr = K_C \int_0^t dt$$

$$\frac{1}{3} (r^3 - r_0^3) = K_C t$$

$$r^3 - r_0^3 = Kt \quad (3.20)$$

Where ‘ $r_0$ ’ is the average radius of the particle at time  $t = 0$

$$K = \frac{8V_m^2 D \sigma C_\infty}{9RT} \quad (3.21)$$

According to Einstein-Stokes equation

$$D = \frac{TK_B}{6\pi\eta r} \quad (3.22)$$

Where,

$K_B$  = Boltzmann constant.

$\eta$  = Viscosity of water.

$r$  = Atomic radius of the particle.

## 3.2 Mathematical model using Solvent-shift method (Keuren et al., 2003).

### 3.2.1 Basic assumptions

- The growth of the particles is a diffusion-limited process.
- Particles are assumed to be spherical.
- Initially the solute concentration is taken to be supersaturated in the bulk.
- Free surface energy is assumed to be neglected.

They have used diffusion equation in spherical coordinates and using mass concentration, they developed the mathematical model. The final equation of the model was

$$t = \frac{3}{4\pi ND} \left[ \frac{1}{6C} \ln \left( \frac{C^3 - X^3}{(C + X)^3} \right) + \frac{1}{\sqrt{3}C} \tan^{-1} \left( \frac{2X - C}{\sqrt{3}C} \right) \right]_{a_0}^a \quad (3.23)$$

$$C = \left[ \frac{3}{4\pi\rho N} (\phi_0 - \phi_{10}) - a_0^3 \right]^{\frac{1}{3}} \quad (3.24)$$

Where,

$N$  = Number density of the particle.

$\rho$  = Density of the solute.

$C$  = Constant.

$a_0$  = Initial particle radius.

$a$  = Final particle radius.

$\phi_{10}$  = Initial bulk concentration.

Then by applying Taylor's series expansion in the equation (3.23) and assuming the initial particle radius and initial bulk concentration to be zero we got,

$$a = \frac{8\pi NDC^3 - 0.4787C^2 + 2C}{19} \quad (3.25)$$

Then by substituting the values of known parameters we can get the particle size with respect to the time.

### 3.3 Sample calculation (LSW approach).

For the calculation of the theoretical values, some assumptions are taken and some derived equations are used by using LSW theory. Then, some datas of particle size and time are generated and compared to the experimental values.

In those three equations (3.20, 3.21, 3.22) some datas are used which are taken from the literature.

$V_m$  = Molar volume of sulfur,  $0.0155 \text{ m}^3 \text{ kmole}^{-1}$

(<http://environmentalchemistry.com/yogi/periodic/S.html>).

$R$  = Universal gas constant,  $8314.3 \text{ kg m}^2 \text{ kmole}^{-1} \text{ s}^2 \text{ K}^{-1}$ .



$T$ =Temperature, 298K.

$K_B$ =Boltzmann constant,  $1.3806 \times 10^{-23} \text{ J K}^{-1}$ .

$r$ =Atomic radius of sulfur,  $109 \times 10^{-12} \text{ m}$

(<http://environmentalchemistry.com/yogi/periodic/S.html>).

$\eta$ =Viscosity of water,  $0.891 \times 10^{-3} \text{ kg m}^{-1} \text{ s}^{-1}$  (at 298K)

([http://www.engineeringtoolbox.com/absolute-dynamic-viscosity-water-d\\_575.html](http://www.engineeringtoolbox.com/absolute-dynamic-viscosity-water-d_575.html)).

$\sigma$ =Surface energy of sulfur,  $40 \times 10^{-3} \text{ J m}^{-2}$  (Chibowski et al., 2008).

$D$ =Diffusion coefficient.

$D$  is calculated by using equation (2) at 298K.

$$D = \frac{TK_B}{6\pi\eta r} = \frac{1.3806 \times 10^{-23} \times 298}{6 \times \pi \times 0.891 \times 10^{-3} \times 109 \times 10^{-12}} = 2.24782 \times 10^{-9} \text{ m}^2 \text{ s}^{-1}$$

$K$ =Coarsening constant.

$K$  is calculated by using equation (1) for the thiosulphate concentration at  $C_\infty=0.5\text{mM}$ , because here I assume that there is 100% conversion of thiosulphate to sulfur and also the total mass of the solute is conserved.

$$K = \frac{8V_m^2 D \sigma C_\infty}{9RT} = \frac{8 \times 0.0155^2 \times 2.24782 \times 10^{-9} \times 40 \times 10^{-3} \times 0.0005}{9 \times 8314.3 \times 298} = 3.8749 \times 10^{-24} \text{ m}^3 \text{ s}^{-1}$$

Here,  $r_0=0$ , because at time ( $t$ ) =0 initial particle radius is zero.

All the above values are substituted in the equation (3). Then with increasing time we got the particle radius and it increases with time. Then those values generated are compared with the experimental values available (Ghosh Chaudhuri, 2009).

### 3.4 Sample calculation (Solvent shift approach).

Here, I assumed that 100 numbers of molecules combine to form nuclei then radius of the nuclei is

$$100 \times \frac{4}{3} \pi r_s^3 = \frac{4}{3} \pi r_n^3$$

$$r_n = (100)^{\frac{1}{3}} \times r_s$$

$$r_n = 5.05933 \times 10^{-10} \text{ m}$$

Where,  $r_s$  = Atomic radius of sulfur.

$r_n$  = Nuclei radius.

Then by applying mass balance and assuming 100% conversion,

$$\text{Density of sulfur} = 2.07 \text{ kg m}^{-3}$$

$$N \times V_n \times 2.07 \times 10^3 \leq 32 \times 10^{-3}$$

$$N \leq 2.85 \times 10^{22}$$

Then by substituting all known values in equation (3.25) we can get the values of radius with respect to time.

# CHAPTER 4

## Results and Discussion

### 4.1 Effect of different parameters on growth kinetics based on LSW Model

#### 4.1.1 Effect of concentration on growth kinetics.

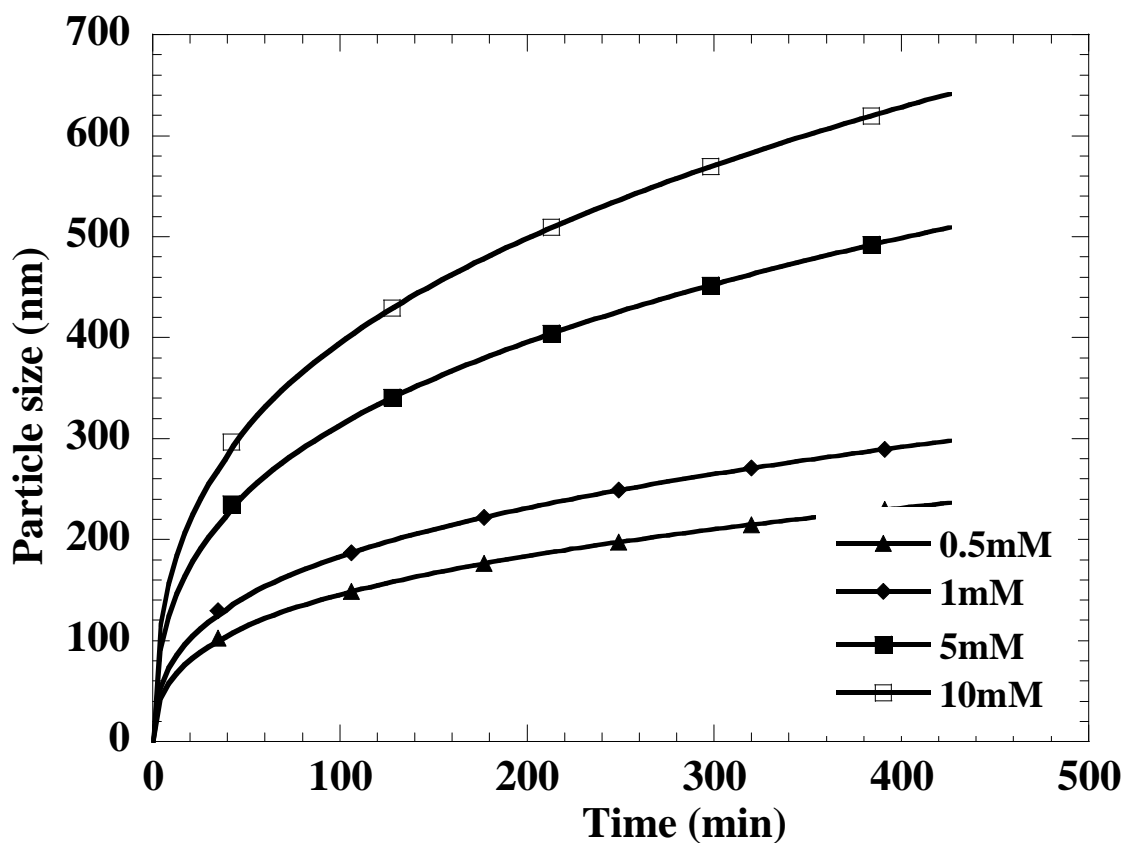


**Fig.4.1. Effect of different reactant concentrations on growth kinetics at 298K.**

In the Fig.4.1, the effects of different reactant concentrations on the particle size are shown. From the plot, it is concluded that with increase in reactant concentration particle growth increases. According to LaMer (1948) rate of the reaction depends on the concentration of the thiosulphate and acid (reactant). This means, with increase in reactant concentration the

density of the nucleate particles also increases. Then, there are more collisions between the particles and due to coarsening the smaller particles gets larger in size by minimizing the energy. Also, as the concentration of particles at the interface increases, the rate of reaction becomes dominated by the diffusion of particles away from the interface. This allows space for the reagents to diffuse to the interface, meet and react. An increase in the transport of reagents to the interface will lead to an increase in the rate of reaction and accordingly growth of the particles increases (Lee et al., 2009). From the above graph it is shown that, for 10mM thiosulphate concentration the growth rate is higher than others and for 0.5mM thiosulphate concentration, the growth rate is very low and it comes to equilibrium quickly. Finally, it is concluded that with increase in reactant concentration the particle size increases.

#### 4.1.2 Effect of temperature on growth kinetics.

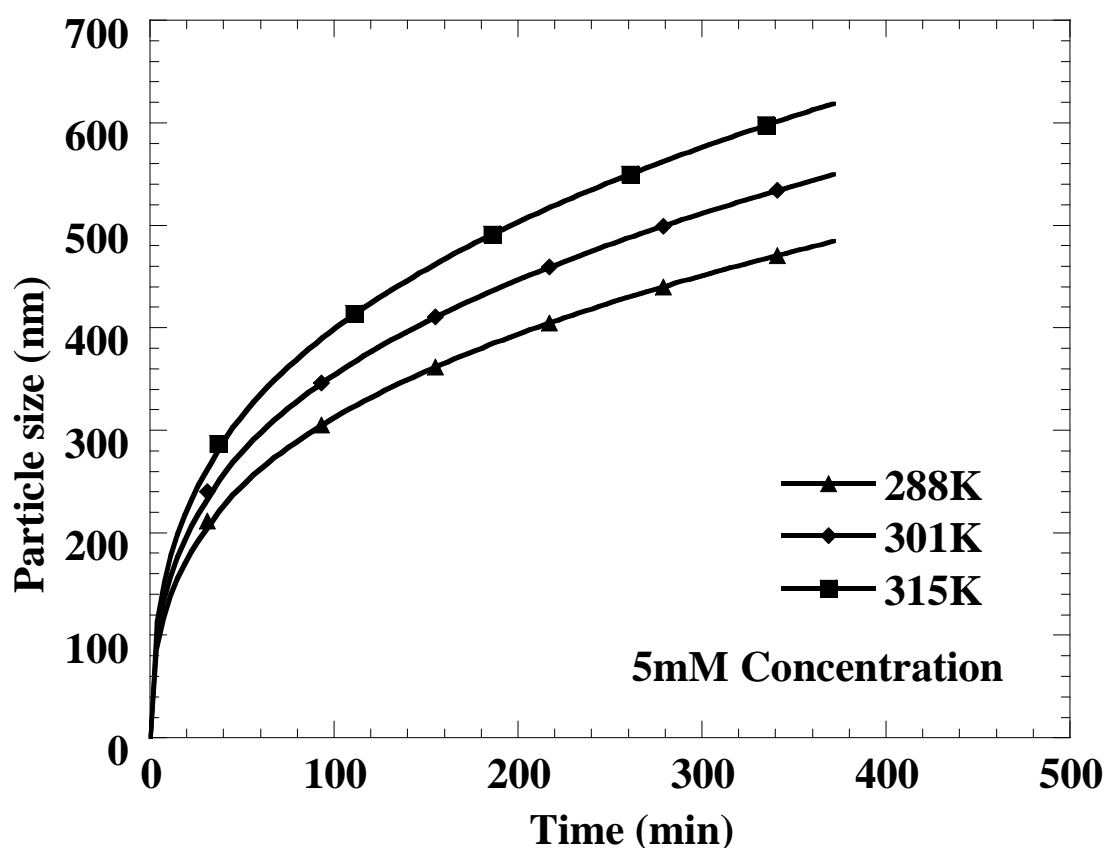


**Fig.4.2. Effects of different temperatures on growth kinetics at 5mM concentration.**

In the Fig.4.2, the effects of different temperature on particle size are shown. Fig.5.2. shows that with increase in temperature particle size increases. The slop of the each curve shows the

growth of the particle at separate temperature. The order of the slop of the each curve at different temperature is,  $315\text{K} > 301\text{K} > 288\text{K}$ . In an endothermic reaction thiosulphate disproportionate to form sulfur and sulfonic acid, so with increase in temperature rate of the reaction increases. With increase in temperature the particles gain more kinetic energy and collision between the particles increases. Due to increase in collision the smaller particles combine rapidly and form larger particles and their size increases due to coarsening. So, it is concluded that with increase in temperature particle size increases.

#### 4.1.3 Effect of surface energy on growth kinetics.

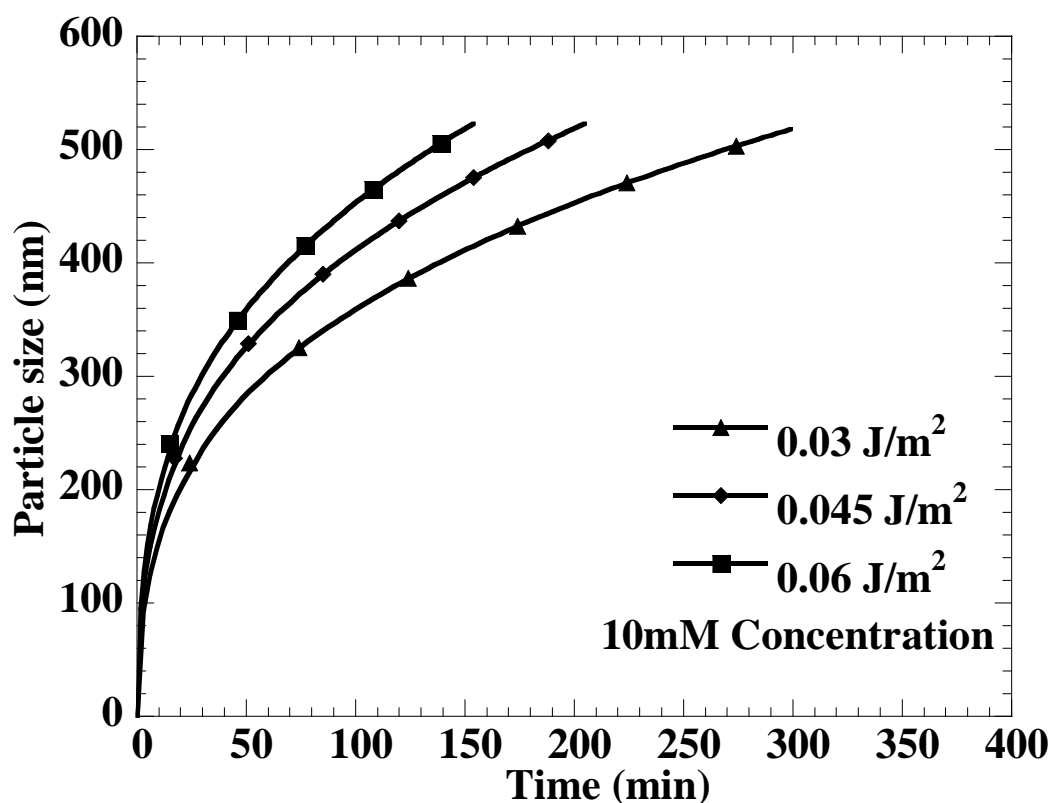


**Fig.4.3. Effect of surface energy on growth kinetics at 10mM concentration.**

In the above plot, effects of surface energy on particle size are shown. The slop of each curve shows the growth of the particle at different surface energy. Figure shows that with increase in surface energy particle size increases also reaction becomes faster. The order of the slop of the curve with different surface energy is  $0.06 > 0.045 > 0.03 (\text{J/m}^2)$ . Fig.5.3. Displays that the curve with surface energy  $0.06 \text{ J/m}^2$  reaches a certain particle size rapidly but the other curves with surface energy  $0.045 \text{ J/m}^2$  and  $0.03 \text{ J/m}^2$  take more time to reach that particle size.

Surface energy means the energy applied to increase the surface area for the interaction of large number of particles and for this reason reaction is very fast with increase in surface energy. Due to the high surface energy the particles are unstable. Then the particles minimize the surface energy by increasing their size and due to this agglomeration also take place. Finally, it is concluded that with increase in surface energy particle size increases and the reaction becomes faster.

## 4.2 Effect of different parameters on growth kinetics based on Solvent-Shifting Model (Keuren et al., 2003).

### 4.2.1 Effect of mass concentration on growth kinetics.

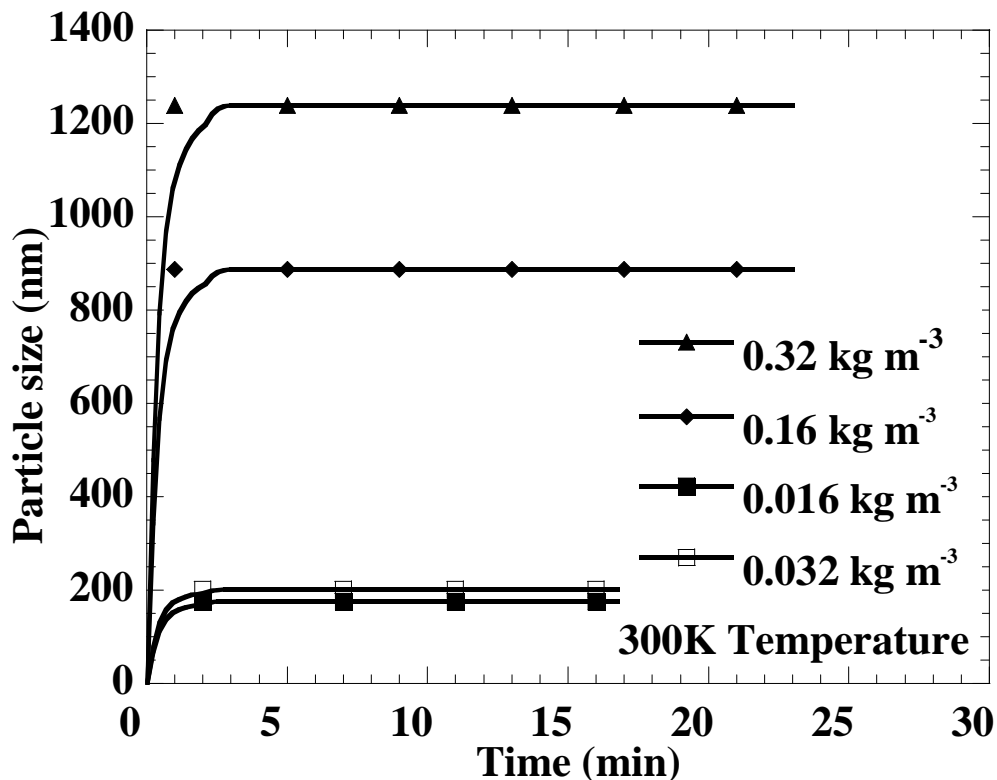


**Fig.4.4. Effect of mass concentration on growth kinetics at 300K temperature.**

In the Fig.4.4, the effect of mass concentration on particle size is shown. Figure shows that with increase in mass concentration particle size increases. Due to increase in mass concentration density of the nucleate molecules increases. So there will be more collision between the molecules and then the smaller particle combine to form the larger particle. So, due to more number of molecules and more collisions the particle having higher mass

concentration acquire bigger size particle than the others. Figure displays that particles having lower mass concentration comes to saturation level very fast. So it is concluded that with increase in mass concentration particle size increases.

#### 4.2.2 Effect of number density on growth kinetics.

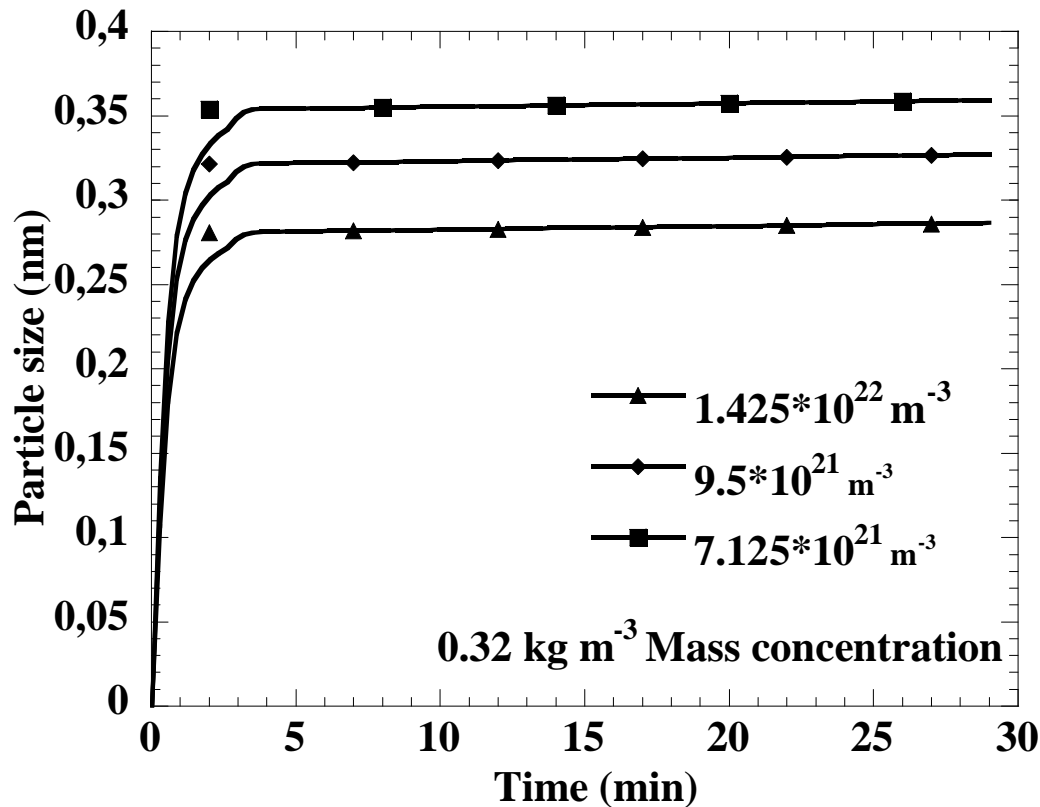


Fig.4.5. Effect of number densities on growth kinetics at 300K temperature.

In the Fig.4.5, the effect of number densities on particle size is shown. Figure shows that with increase in number densities particle size decreases. I have calculated that the limiting number density for 100 molecules to form nuclei is  $2.85 \times 10^{22} \text{ m}^{-3}$ . Then its 1/2, 1/3<sup>rd</sup> and 1/4<sup>th</sup> are taken and compared. From the figure, it is concluded that with increase in number density the particles become finer.

### 4.3 Comparison between experimental and theoretical datas.

#### 4.3.1 Comparison between experimental and theoretical datas of effect of concentration on growth kinetics.

## Discussion

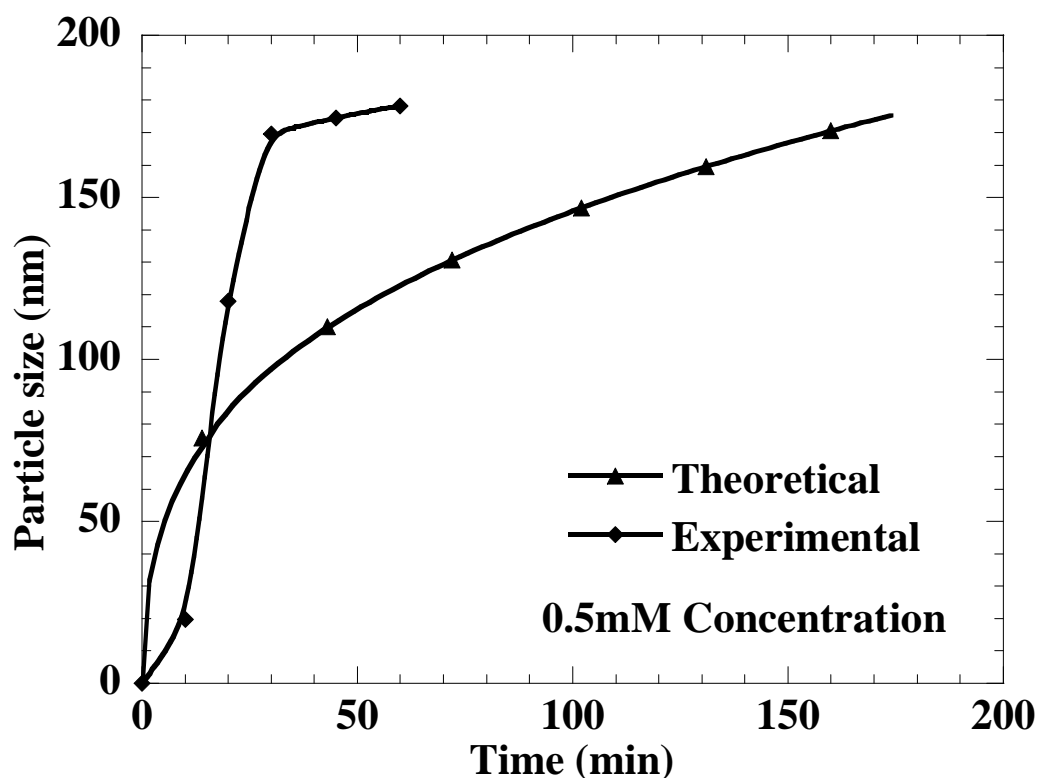


**Fig.4.6. Comparison of the theoretical and experimental effect of 0.5mM reactant concentration on growth kinetics at 298K.**

In the above figure, the comparison between the experimental data and the theoretical data of 0.5mM thiosulphate concentration are shown. The plot is in between time in minute and particle size (diameter) in nanometre. From the plot, it is concluded that the curve of the experimental values is increasing rapidly and then comes to a saturation level after 30 minutes and according to the theoretical values the curve is suddenly increasing upto 10 minutes and then slowly comes to the saturation level, but it will take more time to come to saturation level than the experimental curve as shown in figure.

For 0.5mM concentration the final particle size, according to the experimental values is 178.3nm (Ghosh Chaudhuri, 2009) and from theoretical the final particle size is 175.4nm. The error calculated with respect to the experimental value is 1.6% according to the final particle size but with respect to the time at 60 minutes error is 31%.



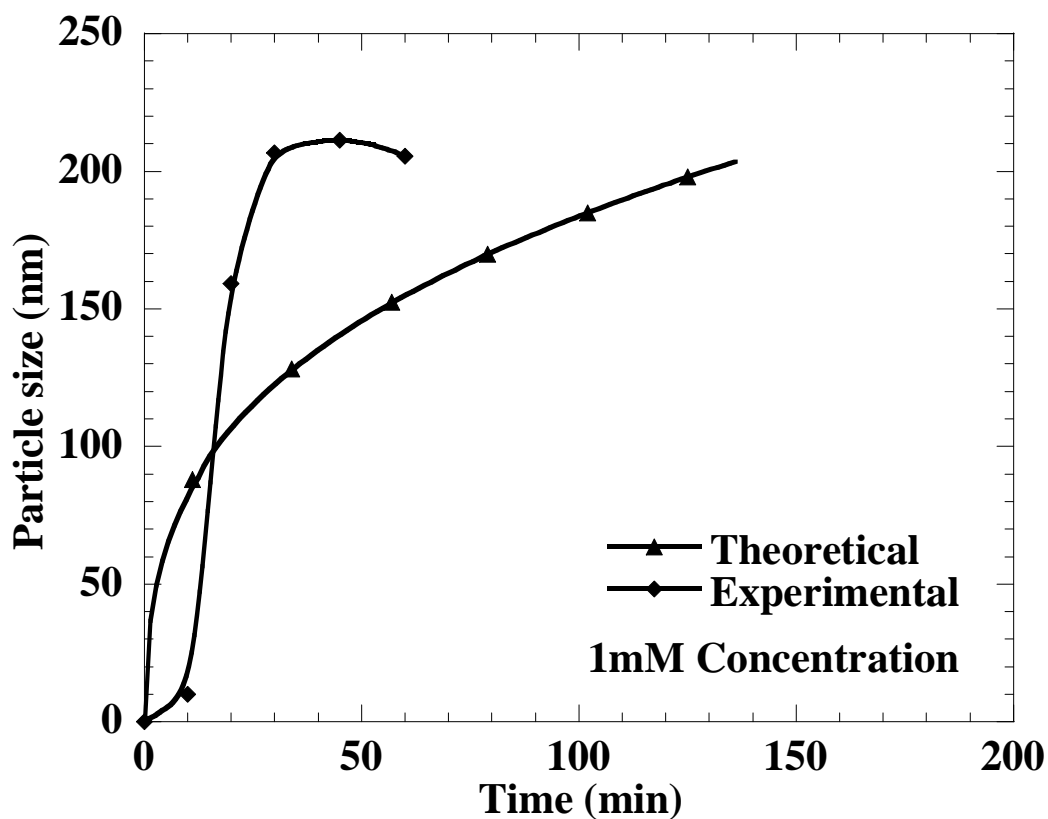


**Fig.4.7. Comparison between theoretical and experimental effect of 1mM reactant concentration on growth kinetics at 298K temperature.**

In the Fig.4.7, the comparison between the experimental datas and the theoretical datas of particle size and time of 1mM thiosulphate concentration are shown. From the plot, it is concluded that the curve of the experimental values is increasing rapidly and then comes to a saturation level after 50 minutes and according to the theoretical values the curve is suddenly increasing more than the experimental curve and cuts the curve at about 70nm particle size and then slowly comes to the saturation level, but it will take more time to come to saturation level than the experimental curve as shown in figure. The particle size calculation is same as before.

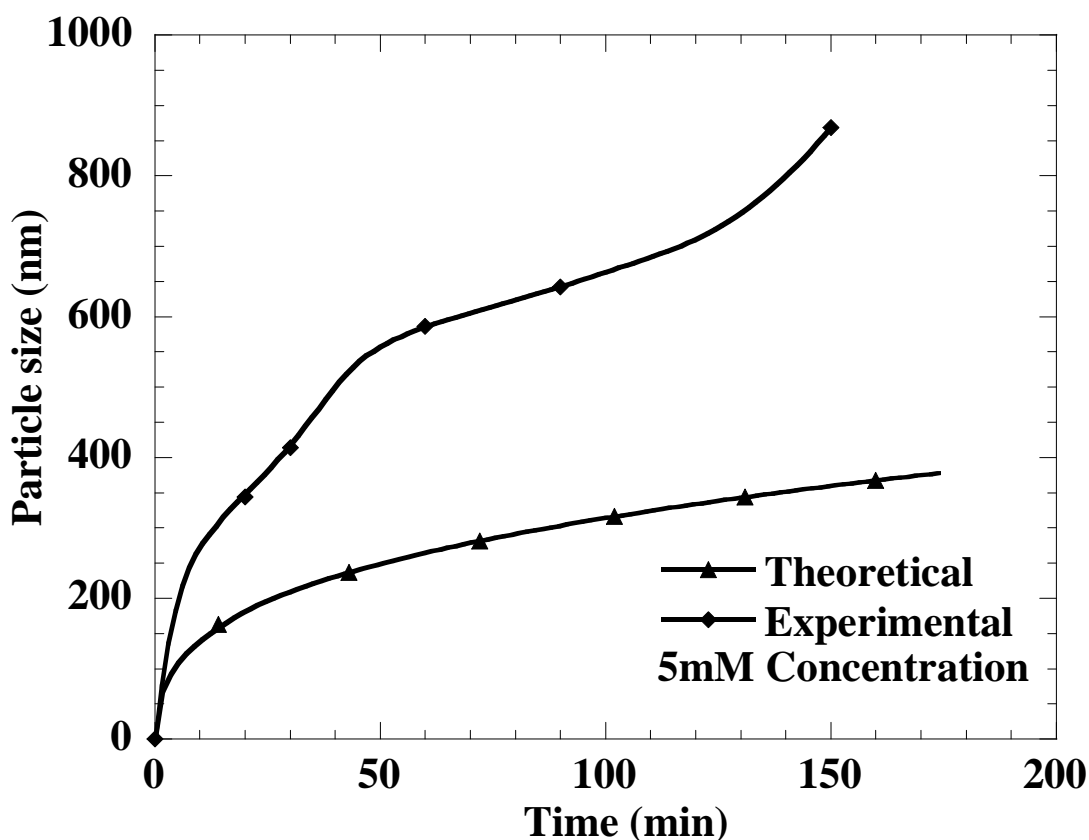


**Fig.4.8. Comparison between experimental and theoretical effect of 5mM concentration on growth kinetics at 298K.**

In the Fig.4.8, the comparison between the experimental datas and the theoretical datas of particle size and time of 5mM thiosulphate concentration are shown. From the plot, it is concluded that the curve of the experimental values is increasing rapidly and then comes to a saturation level after 160 minutes and according to the theoretical values the curve is suddenly increasing with the experimental curve and then slowly comes to the saturation level, but it will take more time to come to saturation level than the experimental curve as shown in figure. The experimental curve reaches the equilibrium at about 890.1nm at 235 minutes and theoretically it. Reaches equilibrium at about 460nm at about 314 minutes, but at 235 minutes the theoretical particle size is 417.6nm. So the error is 48.32% with respect to the final particle size and with respect to time at 235 minutes error is 53%. The particle size calculation is same as before.

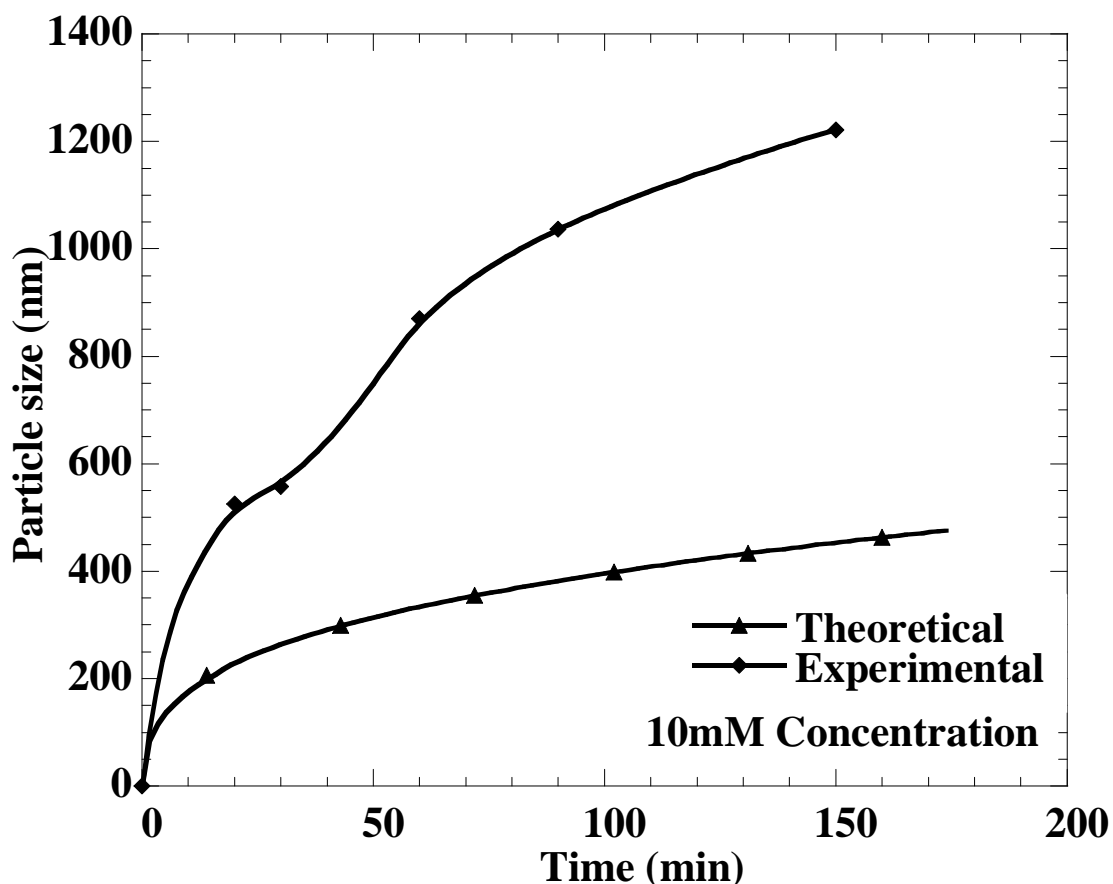


**Fig.4.9. Comparison between experimental and theoretical effect of 10mM reactant concentration on growth kinetics at 298K.**

In the above plot, the comparison between the experimental datas and the theoretical datas of particle size and time of 10mM thiosulphate concentration are shown. From the plot, it is concluded that the curve of the experimental values is increasing rapidly and then comes to a saturation level after 180 minutes and according to the theoretical values the curve is suddenly increasing with the experimental curve upto a size of 160nm and then slowly comes to the saturation level, but it will take more time to come to saturation level than the experimental curve as shown in figure. The experimental curve reaches the equilibrium at about 1239.7nm at 210 minutes and theoretically it reaches equilibrium at about 641.6nm at about 426 minutes, but at 210 minutes the theoretical particle size is 506.8nm. So the error is 48.24% with respect to the final particle size.

### 4.3.2 Comparison between the experimental and theoretical datas of effect of temperature on growth kinetics.

#### Discussion

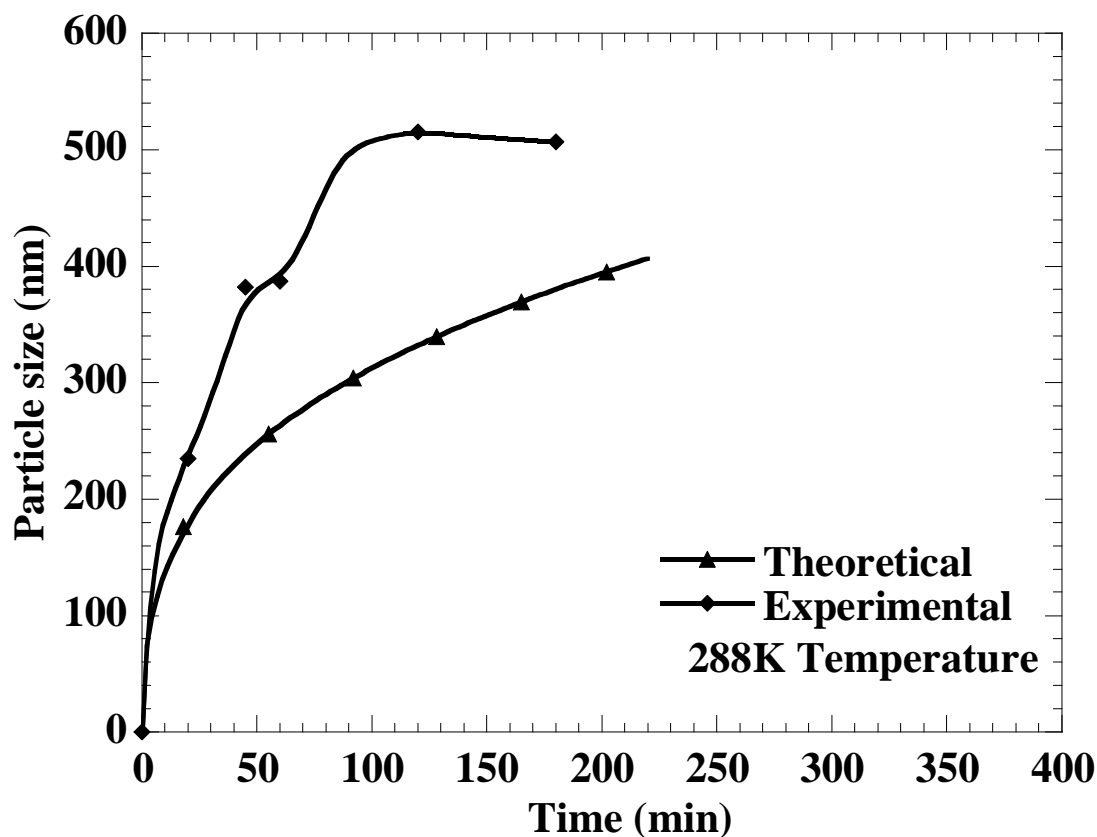


**Fig.4.10. Comparison between experimental and theoretical effect of 288K temperature on growth kinetics at 5mM reactant concentration.**

In the above plot, the comparison between the experimental datas and the theoretical datas of particle size and time at 288K temperature are shown. The plot shows that the experimental curve came to equilibrium at about 180 minutes and the particle size is 506.8nm. According to the theoretical curve it came to saturation slowly than the experimental curve and the time taken is 220 minutes and the particle size is 406.6nm. The error calculated with respect to the final particle is about 19.77%. The calculation of the particle size is same as before by using

equations (1, 2, and 3). Here at different temperatures, surface energy changes and with increase in temperature surface energy increases.

For the calculation surface energy range for sulfur is available (Chibowski et al., 2008). Experimental datas of particle size at different temperatures are available (Ghosh Chaudhuri, 2009).

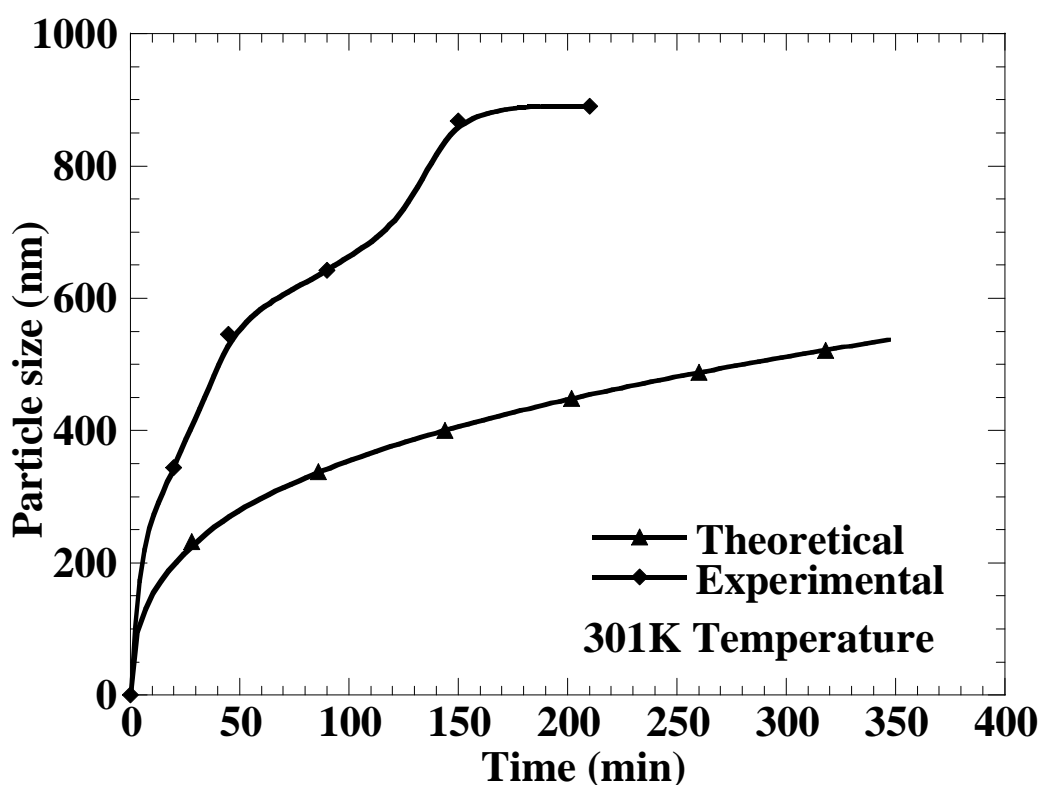


**Fig.4.11. Comparison of experimental and theoretical effect of 301K temperature on growth kinetics at 5mM reactant concentration.**

In the fig.4.11, the comparison between the experimental datas and the theoretical datas of particle size and time at 301K temperature are shown. According to the figure shown the theoretical curve increasing rapidly with the experimental curve upto a height of 120nm and then it slows down to saturation level. The plot shows that the experimental curve came to equilibrium at about 210 minutes and the particle size is 890.1nm. According to the theoretical curve it came to saturation slowly than the experimental curve and the time taken

is 347 minutes and the particle size is 537.05nm. The error calculated with respect to the final particle is about 39.66%.

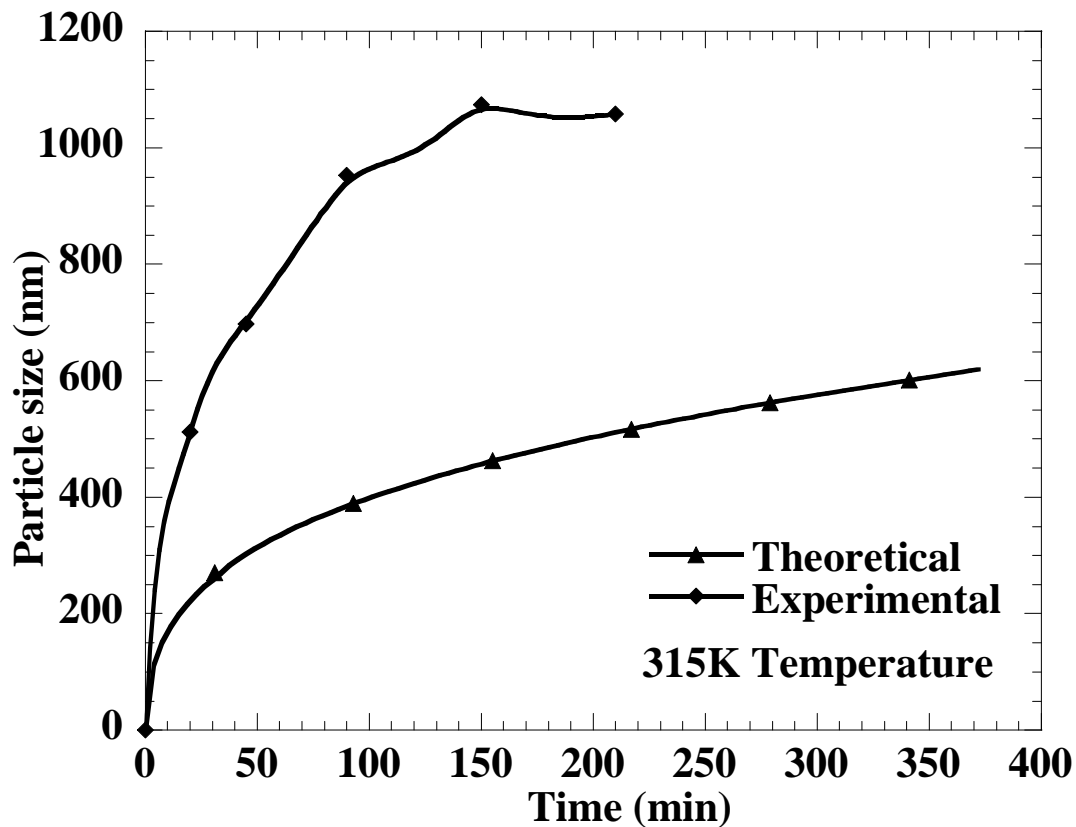


**Fig.4.12. Comparison of experimental and theoretical effect of 315K temperature on growth kinetics at 5mM reactant concentration.**

In the Fig.4.12, the comparison between the experimental datas and the theoretical datas of particle size and time at 315K temperature are shown. The plot shows that the experimental curve came to equilibrium at about 210 minutes and the particle size is 1058nm. According to the theoretical curve it came to saturation slowly than the experimental curve and the time taken is 372 minutes and the particle size is 619nm. The error calculated with respect to the final particle size is about 41.49%.

#### **4.4 Error discussion**

The theoretical data are not properly fitted to the experimental data as shown in the figure may be due to some error in assumptions taken or may be in the experimental data. At first, in the theory, nucleation is neglected and only the coarsening part is shown in the figure, but in the experiment both nucleation and coarsening of the particles occurred. Coarsening is the slowest process and saturation part of the curve and nucleation is the fastest process. In the above figures shown the theoretical data having only the coarsening part is compared with the experimental data having both nucleation and coarsening part. So, due to this there might be some error. Again, we have assumed that there is 100% conversion of thiosulphate to sulfur particle and also the mass of the solute is conserved. For this reason, we have taken that the initial concentration of thiosulphate as the final bulk concentration of the sulfur particle and there is no change in particle concentration, particle concentration is constant from starting to the end. But in the experiment it is not the same because in nucleation stage the particle concentration increases up to critical supersaturation and at growth process particle concentration decreases. So, for this reason there might be some error. Again, in place of hydrodynamic radius we have taken the atomic radius of sulfur because in many papers, hydrodynamic radius was not described in detail and also how to calculate hydrodynamic radius not described in any papers. Generally, hydrodynamic radius is larger than the atomic radius. Due to this also there might be some error. Another factor for which there might be some error is solubility. With increase in temperature solubility we are keeping constant but in some papers it was written that solubility increases with increase in temperature and also particle size increases due to increase in solubility (Segets et al., 2009). Error is calculated theoretical with respect to experimental.

$$\%error = \left| \frac{\text{experimental} - \text{theoretical}}{\text{experimental}} \right| \times 100$$

# CHAPTER 5

## Conclusion

### 5.1 Conclusion.

In this project we have studied the mechanism of formation of sulfur nanoparticles from thiosulphate solution in aqueous media. According to the mechanism every precipitation reaction is followed by nucleation, growth and agglomeration. Nucleation is the very fast stage and then growth is the slowest step and also the rate determining step. After nucleation, the particles having the size more than critical size started growing and the particles having size less than critical size again dissolved in the solution. In this project diffusion is rate determining step. Here we have applied two models that is LSW Model and Solvent-Shifting Model. There were some assumptions we have taken in both the models and then using the equations we have generated the theoretical datas of particle size with respect to time and then we have compared those datas with the experimental datas. From the figures shown in Chapter.5, we concluded that with increase in reactant concentration the particle size increases due to increase in collisions between the particles. Particle size also increases with increase in temperature due increase in kinetic energy and collisions between the molecules. Surface energy also plays a very important role, with increase in surface energy particle size increases and also the growth rate is very fast due to the increase in surface area of the particles which provides the interaction of large number of molecules. The theoretical datas not fitted properly with the experimental datas as shown in Chapter.5, due to some error. The error might be due to some assumptions we have taken that is nucleation was neglected and total mass of the solute is conserved. From the Solvent-Shifting model we have concluded that particle size increases with increase in mass concentration and also increasing number density makes the particle finer.



# References

## Reference

- Buffat, P.; Borel, J.P. Size effect on the melting temperature of gold particle. *J. Phys. Rev.* 1976, A13, 2287-2298.
- Brinker, C.J.; Scherer, G. W. Sol-Gel Science: The Physics and Chemistry of Sol-Gel Processing. Academic Press, 1990, ISBN 0121349705.
- Chibowski, E.; Terpilowski, K. Surface free energy of sulfur—Revisited I. Yellow and orange samples solidified against glass surface. *J. Colloid and Interface Science.* 2008, 319 505–513.
- Choy, J.H.; Jang E.S.; Won J.H.; Chung, J.H.; Jang D.J.; Kim Y.W. Hydrothermal route to ZnO nanocoral reefs and nanofibers. *J. Appl. Phys. Lett.* 2004, 84, 287-289.
- Corriu, R.; Anh, R.T. Molecular Chemistry of Sol-Gel Derived Nanomaterials. John Wiley and Sons. 2009, ISBN 0470721170.
- Deshpande, A.S.; Khomane, R.B.; Vaidya, B.K.; Joshi, R.M.; Harle, A.S.; Kulkarni, B.D. Sulfur Nanoparticle synthesis and characterization from H<sub>2</sub>S gas, using novel biodegradable iron chelate in W/O microemulsion. *J. Nanoscale Research Lett.* 2008, 3, 221-229.
- Destree, C.; Nagy, J.B. Mechanism of formation of inorganic and organic nanoparticles from microemulsions. *J. Advances in Colloid Interface Sci.* 2006, 123-126, 353-367.
- Dierking, I.; Koshbar, L.L.; Afzali-Ardakani, A.; Lowe, A.C.; Held, G.A. Two stage switching behaviour of polymer stabilized cholesteric textures. *J. Apply. Phys.* 1997, 81, 3007-3014.
- Dierking, I.; Koshbar, L.L.; Lowe, A.C.; Held, G.A.; Miller, R.D. *J. Phys. Rev. Lett.* 1997, 79, 3443.
- Ding, J.; Miao, W.F.; McCormick, P.G.; Street, R. Mechanochemical synthesis of ultrafine Fe powder. *J. Appl. Phys. Lett.* 1995, 67, 3804.
- Ellis, M.N.; Ferree, D.C.; Funt, R.C.; Madden, L.V. Effects of an apple scab-resistant cultivar on use patterns of inorganic and organic fungicides and economics of disease control. *J. Plant disease.* 1998, 82, 428-433.

Ethayaraja, M.; Bandyopadhyaya, R. Model for Core-Shell Nanoparticles Formation by Ion-Exchange Mechanism. *J. Ind. Eng. Chem. Res.* 2008, 47, 5982-5985.

Ghosh Chaudhuri, R. Synthesis and Characterization of S@AgBr Core-Shell Nanoparticles. M.Tech. Thesis. 2009, N.I.T, Rourkela, India.

Guo, Y.; Zhao, J.; Yang, S.; Yu, K.; Wang, Z.; Zhang, H. Preparation and characterization of monoclinic sulfur nanoparticles by water in oil microemulsion technique. *Powder Technol.* 2006, 162, 83-86.

Hale, P. S.; Maddox, L. M.; Shapter, J. G.; Voelcker, N. H.; Ford, M. J.; Waclawik, E. R. Growth Kinetics and Modelling of ZnO Nanoparticles. *J. Chemical Education.* 2005, 82, 775-778.

Keuren, E. V.; Georgieva, E.; Durst, M. Kinetics of the Growth of Anthracene Nanoparticles. *J. Dispersion Sci. Technol.* 2003, 24, 721-729.

Klein, L. Sol-Gel Optics: Processing and Applications. Springer Verlag. 1994, ISBN 0792394240.

Koch, C.C.; Cho, Y. S. Nanocrystals by high energy ball milling. *J. Nanostructured Mater.* 1992, 1, 207-212.

LaMer, V. K.; Kenyon, A. S. Kinetics of the mono dispersed sulfur solution from thiosulphate and acid. *J. Colloidal Sci.* 1947, 2, 257-264.

LaMer, V. K.; Denegar, R. H. Theory, production and mechanism of formation of mono dispersed hydrosols. *J. Am. Chem. Soc.* 1950, 72, 4847-4854.

LaMer, V. K. Nucleation in phase transition. *J. Ind. Eng. Chem.* 1952, 44, 1270-1277.

LaMer, V.K.; Turgeon, J.C. The Kinetics of the Formation of the Carbinol of Crystal Violet. *J. Am. Chem. Soc.* 1952, 74, 5988-5994.

LaMer, V.K.; Umberger, J.Q. The Kinetics of Diffusion Controlled Molecular and Ionic Reactions in Solution as Determined by Measurements of the Quenching of fluorescence. *J. Am. Chem. Soc.* 1945, 67, 1099-1109.

Lee, W. P.; Chen, H.; Dryfe, R.; Ding, Y. Kinetics of nanoparticle synthesis by liquid-liquid interfacial reaction. *Colloids Surf. A* 2009, 343, 3-7.

Lifshitz, I.M.; Slyozov, V.V. The kinetics of precipitation from supersaturated solid solutions. *J. Phys. Chem. Solids.* 1961, 19, 35-50.

- McCormick, P.G.; Tsuzuki, T.; Robinson, J.S.; Ding, J. Nanopowders synthesized by mechanochemical processing. *J. Adv. Mater.* 2001, 13, 1008-1010.
- Oskam, G.; Nellore, A.; Penn, R. L.; Searson, P. C. The Growth Kinetics of TiO<sub>2</sub> Nanoparticles from Titanium(IV) Alkoxide at High Water/Titanium Ratio. *J. Phys. Chem. B.* 2003, 107, 1734-1738.
- Rajaram, C.V.; Hudson, S.D.; Chien, L.C. Morphology of Polymer-Stabilized Liquid Crystals. *J. Chem. Mater.* 1995, 7, 2300-2308.
- Rajaram, C.V.; Hudson, S.D.; Chien, L.C. Morphology of dia-crylate copolymer networks formed in liquid crystalline media. *Polymer.* 1998, 39, 5315-5319.
- Rao, C.N.R.; Muller, A.; Cheetham, A.K. Nanomaterials Chemistry Recent Developments and directions. WILEY-VCH Verlag GmbH & Co. 2007, 140-144.
- Robert, J.C.; Basu, T.K. Sulfur: its clinical and toxicologic aspects. *J. Nutrition.* 2003, 19, 54-61.
- Sarkar, D.; Gupta, P.; Gautam, A.; Khilar, K.C. Reuse of surfactant/oil phase in nanoparticles synthesis using W/O microemulsion. *AIChE.* 2008, 54(2), 582-587.
- Segets, D.; Gradl, J.; Taylor, R. K.; Vassilev, V.; Peukert, W. Analysis of Optical Absorbance Spectra for the Determination of ZnO Nanoparticle Size Distribution, Solubility, and Surface Energy. *J. Am. Chem. Soc.* 2009, 3, 1703-1710.
- Seokwon, K.; Roman, K.; Musah, R.A. Antibacterial and antifungal activity of sulfur containing compounds from *petiberia alliacea L.* *J. Ethnopharmacology.* 2006, 104, 188-192.
- Shaffer, G.B.; McCormick, P.G. Nanopowders synthesized by Mechanochemical processing. *J. Mater. Sci. Lett.* 1990, 9, 1014-1016.
- Shukla, D.; Mehra, A. Modeling shell formation in core-shell nanocrystals in reverse micelle systems. *Langmuir.* 2006, 22, 9500-9506.
- Sugimoto, T. Preparation of monodispersed colloidal particles. *Adv. Colloid Interface Sci.* 1987, 28, 65-108.
- Takacs, L. Multiple Combustion Induced by Ball Milling. *J. Appl. Phys. Lett.* 1996, 69, 436-438.
- Tojo, C.; Barroso, F.; Dios, M. Critical nucleus size effects on nanoparticle formation in microemulsions. *J. Colloid Interface Sci.* 2006, 296, 591-598.

Wagner, C. Theory of precipitate change by redissolution. *J. Z. Elektrochem.* 1961, 65, 581-591.

Wong, E. M.; Bonevich, J. E.; Searson, P. C. Growth Kinetics of Nanocrystalline ZnO Particles from Colloidal Suspensions. *J. Phys. Chem. B* 1998, 102, 7770-7775.

Xie, X.Y.; Zheng, W.J.; Bai, Y.; Liu, J. Cystine modified nanosulfur and its spectral properties. *J. Mater. Lett.* 2009, 63, 1374-1376.

Yang, H.; McCormick, P.G. Mechanochemical Processing. *J. Metall. Mater. Trans.* 1998, 29B, 449-445.

[http://www.engineeringtoolbox.com/absolute-dynamic-viscosity-water-d\\_575.html](http://www.engineeringtoolbox.com/absolute-dynamic-viscosity-water-d_575.html).

<http://environmentalchemistry.com/yogi/periodic/S.html>.